# VELOCITY DISTRIBUTION IN TRAPEZOIDAL MEANDERING CHANNEL

*A thesis submitted to*

*National Institute of Technology, Rourkela*

*In partial fulfillment for the award of the degree*

*of*

**Master of Technology in Civil Engineering**

**With specialization in**

**Water Resources Engineering**

**By**

**Laxmipriya Mohanty (211CE4252)**

**Under the supervision of**

**Professor K.C. Patra**


**Department of Civil Engineering**

**National Institute of Technology, Rourkela**

**Odisha-769008**

**May 2013**

**DEPARTMENT OF CIVIL ENGINEERING**
**NATIONAL INSTITUTE OF TECHNOLOGY, ROURKELA**

## DECLARATION

I hereby declare that this submission is my own work and that, to the best of my knowledge and belief, it contains no material previously published or written by another person nor material which to a substantial extent has been accepted for the award of any other degree or diploma of the university or other institute of higher learning, except where due acknowledgement has been made in the text.

**LAXMIPRIYA MOHANTY**

**DEPARTMENT OF CIVIL ENGINEERING**
**NATIONAL INSTITUTE OF TECHNOLOGY, ROURKELA**

# CERTIFICATE

This is to certify that the thesis entitled **"Velocity Distribution in Trapezoidal Meandering Channel"** is a bonafide record of authentic work carried out by **Laxmipriya Mohanty** under my supervision and guidance for the partial fulfillment of the requirement for the award of the degree of Master of Technology in hydraulic and Water Resources Engineering in the department of Civil Engineering at the National Institute of Technology, Rourkela.

The results embodied in this thesis have not been submitted to any other University or Institute for the award of any degree or diploma.

**Date:**

**Place: Rourkela**

**Prof. K.C. Patra**
Department of Civil Engineering
National Institute of Technology, Rourkela
Rourkela-769008


# ACKNOWLEDGEMENTS

I am deeply indebted to **National Institute of Technology, Rourkela** for providing me the opportunity to pursue my Master's degree with all necessary facilities.

I take this opportunity to express my sincere and profound gratitude towards my guide **Prof. K.C Patra** whose whole hearted support, timely encouragement in every stage of this work has been the real cause to shape the work in present form. I would also like to thank **Prof. KK Khatua** to boost my confidence during my low times and providing me potential helps without whom this project might not be a successful one.

I would like to extend my thanks to all professors of Water Resources department for their valuable help they have provided when I was in need. I am also thankful to staff members and students associated with the Fluid Mechanics and Hydraulics Laboratory of Civil Engineering Department, especially Mr. P. Rout for his useful assistance and cooperation during the entire course of the experimentation and helping me in all possible ways.

I wish to thank all of my fellow classmates for their kind help and co-operation extended during my course of study.

Lastly I thank my parents for their overall support and encouragement.

Date: LAXMIPRIYA MOHANTY

## ABSTRACT

Analysis of fluvial flows are strongly influenced by geometry complexity and large overall uncertainty on every single measurable property, such as velocity distribution on different sectional parameters like width ratio, aspect ratio and hydraulic parameter such as relative depth. The geometry selected for this study is that of a smooth sine generated trapezoidal main channel flanked on both sides by wide flood plains. The parameters which were changed in this research work include the overbank flow depth, main channel flow depth, incoming discharge of the main channel and floodplains.

This paper presents a practical method to predict lateral depth-averaged velocity distribution in trapezoidal meandering channels. Flow structure in meandering channels is more complex than straight channels due to 3-Dimentional nature of flow. Continuous variation of channel geometry along the flow path associated with secondary currents makes the depth averaged velocity computation difficult. Design methods based on straight-wide channels incorporate large errors while estimating discharge in meandering channel. Hence based on the present experimental results, a nonlinear form of equation involving 3 parameters for estimating lateral depth-averaged velocity is formulated. The present experimental meandering channel is wide (aspect ratio = b/h > 5) and with high sinuosity of 2.04. A quasi1D model Conveyance Estimation System (CES) was then applied in turn to the same compound meandering channel to validate with the experimental depth averaged velocity. The study serves for a better understanding of the flow and velocity patterns in trapezoidal meandering channel.

A commercial code, ANSYS-CFX 13.0 is used to simulate a 60 meander channel using Large Scale Eddy (LES) model. Contours regarding the velocities in three directions are derived.



***Keywords:*** Aspect Ratio; *Compound Channel;* CES; *Depth averaged velocity*; *Discharge; Flow depth; Meandering channels; Secondary currents.*

## CONTENTS

**Page No.**

# LIST OF TABLES

# LIST OF FIGURES AND PHOTOGRAPHS

## NOTATIONS

| | |
|---|---|
| $Q_a$ | Actual discharge; |
| $C_d$ | Coefficient of discharge calculated from notch calibration = 0.74; |
| $C_r$ | Courant number; |
| $C_s$ | Smagorinsky constant; |
| $L$ | Length of the notch; |
| $H_n$ | Height of water above the notch; |
| $g$ | Acceleration due to gravity; |
| l | Length scale of unresolved motion; |
| b | Channel base width; |
| $d$ | Outside diameter of the probe; |
| G | Gaussian filters; |
| $H$ | In bank depth of flow; |
| $H'$ | Over bank depth of flow; |
| $k$ | Turbulent kinetic energy; |
| $P$ | Wetted perimeter; |
| $R$ | Hydraulic radius; |
| $Y,h$ | Main channel bank full depth; |
| $S_r$ | Sinuosity; |
| s | Bed slope of the channel; |
| $S_{ij}$ | Resolved strain rate tensor; |
| U | Longitudinal point velocity; |
| $\|z-z_{toe}\|$ | Lateral distance from the toe of slope to the point of interest (positive going towards edge of water and negative over the channel bed); |

| | |
|---|---|
| y | Lateral distance; |
| $Z$ | Cotangent of bank slope; |
| $U(z)$ , $U_d$ | Depth-averaged velocity; |
| $U^*$ | Cross-sectional averaged velocity; |
| $U_d/U^*$ | Normalised Depth-averaged velocity |
| x | $(\pm\lvert z-z_{toe}\rvert/YZ)$; |
| $\alpha$ | Aspect ratio; |
| $\rho$ | Fluid density; |
| $\theta$ | Angle between channel bed and horizontal; |
| $\nu$ | Kinematic viscosity; |
| $\varepsilon$ | Turbulent kinetic energy dissipation rate; |
| $\omega$ | Specific dissipation; |
| $\sigma_{ij}$ | Normal stress component on plane normal to i along j; |
| $\tau_{ij}$ | Shear stress component on plane normal to i along j; |
| $\bar{u}_i'$, $\bar{u}_j'$ | Time averaged instantaneous velocity component along i,j directions |
| $\mu$ | Coefficient of dynamic viscosity; |
| $\Delta h$ | Difference between dynamic and static head; |

**Subscripts**

| | |
|---|---|
| *a* | actual |
| *b, bed* | bed |
| *d* | depth average |
| r | relative |
| *t* | theoretical |
| *w* | wall |
| *mod.* | modelled |
| *i, j, k* | *x, y, z* directions respectively |
| *i, inner* | inner bank or wall of meandering channel |
| *o, outer* | outer bank or wall of meandering channel |
| * | mean |

# INTRODUCTION

## 1.1 Overview of Meandering Channels

River is the author of its geometry. The river network is an open system always tending towards equilibrium and the hydraulically interdependent factors such as velocity, depth, channel width and slope mutually interact and self adjust to accommodate the changes in river plan form geometry and discharge contributed by drainage basin. Straightness of rivers is a temporary state, the more usual and stable state whereas a meander is characterized by lower variances of hydraulic factors. Therefore not a single natural river possesses a straight geometry. Almost all natural rivers meander. In fact Straight River reaches longer than 10 to 12 times the channel widths are non existence in nature.

A **meander**, in general, is a bend in a sinuous watercourse or river. A meander is formed when the moving water in a stream erodes the outer banks and widens its valley. As the inner part of the river has less energy it deposits what it is carrying. As a result a snaking pattern is formed, the stream back and forth across its down axis valley. Also second reason of formation of meander as suggested by Leopold (1996) is the secondary circulation in the cross sectional plane. As Leliavsky (1955) describes the second phenomenon of river meandering in his book which quotes "The centrifugal effect, which causes the super elevation may possibly be visualized as the fundamental principles of the meandering theory, for it represents the main cause of the helicoidal crosscurrents which removes the soil from the concave banks, transport the eroded material across the channel, and deposit it on the convex banks, thus intensifying the tendency towards meandering. It follows therefore that the slightest accidental irregularity in channel formation, turning as it does, the streamlines

from their straight course may, under certain circumstances constitute the focal point for the erosion process which leads ultimately to meander".

The two critical parameters that govern the flow in open meandering channel are sinuosity and least centreline radius ($r_c$) to channel width ($b$) ratio. Sinuosity defines how much a river course deviates from shortest possible path (how much it meanders). the sinuosity index is 1 for straight channels whereas for meandering channels it is greater than 1 and can increase to infinity for a closed loop (where the shortest path length is zero) or for an infinitely-long actual path. Meandering channels are also classified as shallow or deep depending on the ratio of the average channel width (b) to its depth (h). In shallow channels (b/h'>5, Rozovskii, 1961) the wall effects are limited to a small zone near the wall which may be called as "wall zone". The central portion called "core zone" is free from the wall effects. Whereas in deep channels (b/h'<5) the influence of walls are felt throughout the channel width. However meandering channels are still a subject of research which involves numerous flow parameters that are intricately related giving rise to complex three dimensional motions in the flow. Due to this the 1 D and 2D modeling of open channel flows fail to estimate the discharge precisely. So a paradigm shift is towards the study of three dimensional modelling of open channel flows that can capture and take into account the complicated unseen phenomena called *"turbulence"*.

**1.2 Velocity Distribution in Open Channels**

The knowledge of velocity distribution helps to know the velocity magnitude at each point across the flow cross-section. It is also essential in many hydraulic engineering studies involving bank protection, sediment transport, conveyance, water intakes and geomorphologic investigation. Despite several researches on various aspects of velocity distributions in curved meander rivers, no systematic effort has yet been made to establish the

relationship between the dominant meander wavelength, discharge and the velocity distributions. In straight channel velocity distribution varies with different width-depth ratio, whereas in meandering channel velocity distribution varies with aspect ratio, sinuosity, meandering making the flow more complex to analyze. Compound channels are all the way different and velocity distribution is a combination of flood plain and main channel (straight or meandering). In laminar flow max stream wise velocity occurs at water level; for turbulent flows, it occurs at about 5-25% of water depth below the water surface (Chow, 1959). Typical stream wise velocity contour lines (isovels) for flow in various cross sections are shown in Fig. 1.1.

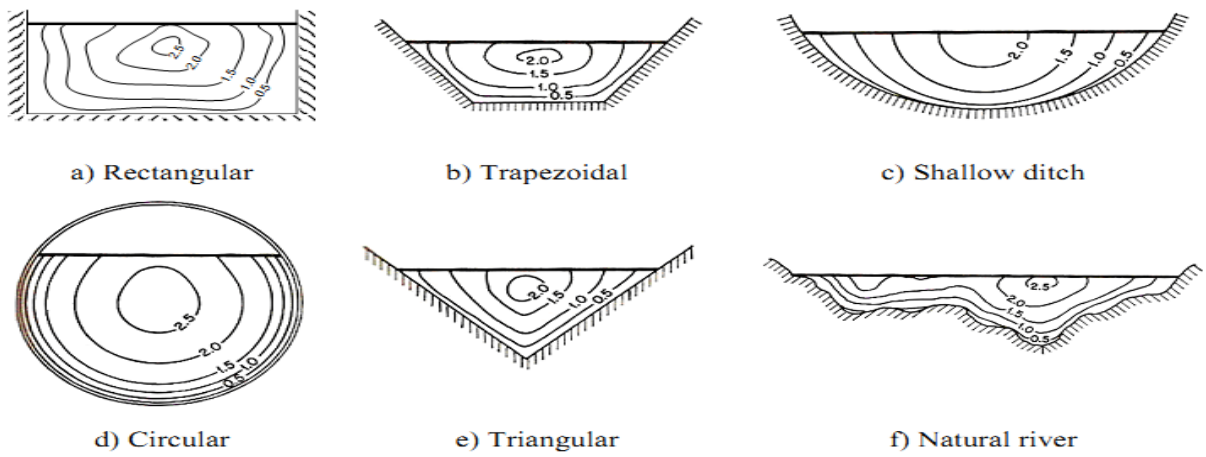


**Fig.1.1 Contours of constant velocity in various open channel sections (Chow, 1959)**

### 1.2.1 Logarithmic law

The "logarithmic law" formulation for the velocity profile in turbulent open channel flow is based on Prandtl's (1926) theory of the "law of the wall" and the "boundary layer" concept. The boundary layer is a thin region of fluid near a solid surface (bed or wall) where the boundary resistance and the viscous interactions affect the fluid motion and subsequently, the velocity distribution. In the fully developed flow region, this layer includes two main sub-layers. Near the solid boundary, a viscous sub-layer (laminar layer) forms where the viscous

force is predominant. In contrast, further away from the boundary, the turbulent shear stresses play a major role in the defect layer (turbulent layer).

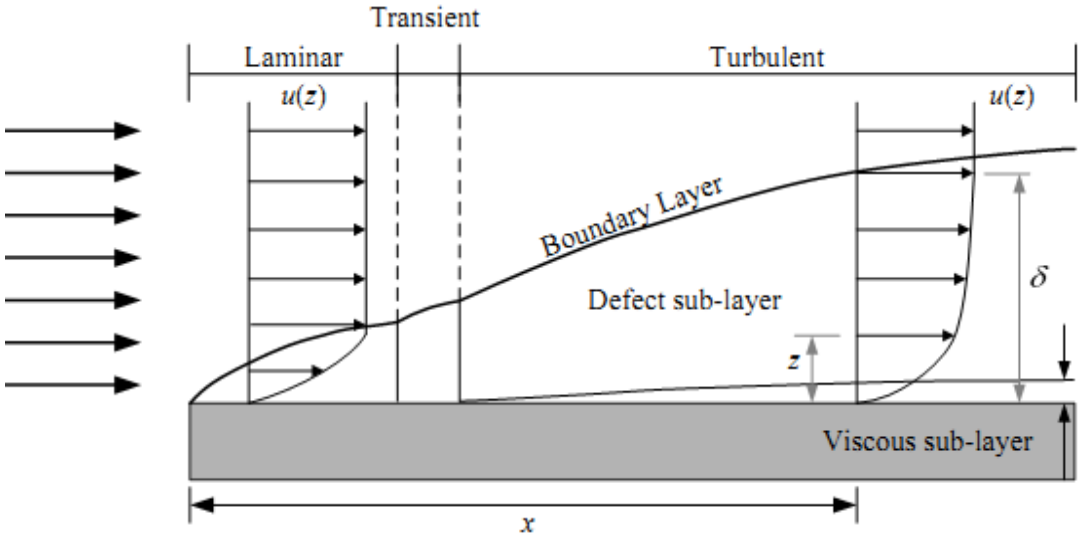


**Fig. 1.2 External fluid flow across a flat plate (after Massy, 1998)**

The "law of the wall" states that the in the stream wise direction, the average fluid velocity in the boundary layer varies logarithmically with distance from the wall surface.

### 1.2.2 Power law

An alternative function for the velocity distribution is the "power law". The general form of this law is proposed as (Barenblatt and Prostokishin, 1993; Schlichting, 1979):

$u_+ = C_4(z^+)^m$ , where $C_4$ and m are the coefficient and exponent of the power law.

### 1.2.3 Chiu's velocity distribution

An alternative approach from the stated empirical velocity distribution equations is the method developed by Chiu (1987, 1989). Based on the probability concept and entropy maximization principle, Chiu derived a new two-dimensional equation for the velocity field. This equation is capable of describing the variation of velocity in both vertical and transverse directions with the maximum velocity occurring on or below the water surface. It can also

accurately describe the velocity distribution in regions near the water surface and channel bed, where most the existing measuring devices face problems.

### 1.3 Depth-Averaged Velocity

It is quite difficult to model flows in meandering trapezoidal channel as the inner and outer banks exert unequal shear drag on the fluid flow that ultimately controls the depth- averaged velocity. Depth-averaged velocity means the average velocity for a depth 'h' is assumed to occur at a height of 0.4h from the bed level.

#### 1.3.1 AIM OF PRESENT RESEARCH

It is concluded from literature review that very less work has been done regarding lateral distribution of depth-averaged velocity in meandering trapezoidal channel. However lack of qualitative and quantitative experimental data on the depth averaged velocity in meandering channels is still a matter of concern. The present study aims at collecting velocity data from wide meandering channel trapezoidal at cross section. The objective of the present work is listed as:

- To study the distribution of stream wise depth-averaged velocity at channel bend apex for single flow depth. Also to study its variation at different flow depths for in bank and overbank flow conditions.
- To propose equations for simple meandering channel trapezoidal at cross section to fit experimental data.
- To validate the depth averaged velocity data with quasi one dimensional model Conveyance Estimation System (CES) for overbank flow conditions.
- To simulate a 60 degree simple meandering channel using Large Eddy Simulation (LES) model and to derive 3 dimensional velocity contours for the same.

## 1.4 ORGANISATION OF THESIS

The thesis consists of seven chapters. General introduction is given in Chapter 1, literature survey is presented in Chapter 2, experimental work is described in Chapter 3, experimental results are outlined in Chapter 4 and analysis based on experimental results are done in Chapter 5, Chapter 6 comprises numerical modelling and finally the conclusions and references are presented in Chapter 7.

General view on rivers and flooding is provided at a glance in the first chapter. Also the chapter introduces the concept of velocity distribution in meandering channels. It gives an overview of numerical modelling in open channel flows.

The detailed literature survey by many eminent researchers that relates to the present work from the beginning till date is reported in chapter 2. The chapter emphasizes on the research carried out in straight and meandering channels for both in bank and overbank flow conditions based on velocity distribution.

Chapter three describes the experimental programme as a whole. This section explains the experimental arrangements and procedure adopted to obtain observation at different points in the channel. Also the detailed information about the instrument used for taking observation is given.

The experimental results regarding stage-discharge relationship, velocity for in bank and overbank flow conditions and depth average velocity are outlined in chapter four. Also this chapter discusses the technique adopted for measuring depth average velocity.

Analyses of the experimental results are done in Chapter 5. The analysis of depth average velocity distribution pattern for in bank and overbank flow conditions is presented in this chapter.

Chapter six presents significant contribution to numerical simulation of in bank channels. The numerical model and the software used within this research are also discussed.

Finally, chapter seven summarizes the conclusion reached by the present research and recommendation for the further work is listed out.

References that have been made in subsequent chapters are provided at the end of the thesis.

# REVIEW OF LITERATURE

## 2.1 OVERVIEW

Distribution of flow velocity in longitudinal and lateral direction is one of the important aspects in open channel flows. It directly relates to numerous flow features like water profile estimation, shear stress distribution, secondary flow, channel conveyance and host to other flow entities. Various factors that affect the velocity distribution such as channel geometry, types and patterns of channel, channel roughness and sediment concentration in flow has been critically studied by many eminent researchers in the past. Prandtl (1932) developed the general form of velocity distribution, which is generally considered as P-vK law, this law was derived by assuming the "shear stress is constant", and can be applied near bed, but has been applied in outer flow region with modification of von karman constant like Milikan(1939) , Vanoni (1941). The P-vK law was derived by taking shear stress as constant whereas the shear stress is not constant in turbulent layer (outer zone) in open channel flow. Milikan (1939) suggested that actual velocity distribution consists of logarithmic part and correction part, where the correction part considers the outer layer into account. So detailed literature review is done for four different channel types followed by works on numerical modelling for open channel flows.

## 2.2 PREVIOUS EXPERIMENTAL RESEARCH ON VELOCITY DISTRIBUTION

### 2.2.1 STRAIGHT SIMPLE CHANNEL

Coles (1956) proposed a semi-empirical equation of velocity distribution, which can be applied to outer region and wall region of plate and open channel. He generalized the logarithmic formula of the wall with tried wake function, w(y/8).This formula is asymptotic to the logarithmic equation of the wall as the distance y approaches the wall. This is basic formulation towards outer layer region.

Coleman (1981) proposed that the velocity equation for sediment-laden flow consists of two parts, as originally discussed by Coles for clear-water flow. Also he has revealed that the von Karman coefficient is independent of sediment concentration. The elevation of the maximum velocity and the deviation of velocity from the logarithmic formula at the water surface are functions of the aspect ratio of the channel. The log-law is developed into an equation applicable to the whole flow including the region near the water surface for various boundary conditions. The wake law describes the velocity distribution below the maximum velocity point.

M. Salih Kirkgoz *et al*. (1997) measured mean velocities using a Laser Doppler Anemometer (LDA) in developing and fully developed turbulent subcritical smooth open channel flows. From the experiments it is found that the boundary layer along the centre line of the channel develops up to the free surface for a flow aspect ratio $b/h \geq 3$. In the turbulent inner regions of developing and fully developed boundary flows, the measured velocity profiles agree well with the logarithmic "law of the wall" distribution. The "wake" effect becomes important in the velocity profiles of the fully developed boundary layers.

Sarma *et al*. (2000) tried to formulate the velocity distribution law in open channel flows by taking generalized version of binary version of velocity distribution, which combines the logarithmic law of the inner region and parabolic law of the outer region. The law developed by taking velocity-dip in to account.

Wilkerson *et al*. (2005) using data from three previous studies, developed two models for predicting depth-averaged velocity distributions in straight trapezoidal channels that are not wide, where the banks exert form drag on the fluid and thereby control the depth-averaged velocity distribution. The data they used for developing the model are free from the effect of secondary current. The 1$^{st}$ model required measured velocity data for calibrating the model coefficients, where as the 2$^{nd}$ model used prescribed coefficients. The 1$^{st}$ model is

recommended when depth-averaged velocity data are available. When the 2nd model is used, predicted depth-averaged velocities are expected to be within 20% of actual velocities.

Knight *et al*. (2007) used Shiono and Knight Method (SKM), which is a new approach to calculating the lateral distributions of depth-averaged velocity and boundary shear stress for flows in straight prismatic channels, also accounted secondary flow effect. It accounts for bed shear, lateral shear, and secondary flow effects via3 coefficients- f, λ, and Γ —thus incorporating some key 3D flow feature into a lateral distribution model for stream wise motion. This method used to analyze in straight trapezoidal open channel. The number of secondary current varies with aspect ratio. It is three for aspect ratio less than equal to 2.2 and four for aspect ratio greater than equal 4.

Afzal *et al*. (2007) analyzed power law velocity profile in fully developed turbulent pipe and channel flows in terms of the envelope of the friction factor. This model gives good approximation for low Reynolds number in designed process of actual system compared to log law.

Yang (2010) investigate depth-average shear stress and velocity in rough channels. Equations of the depth-averaged shear stress in typical open channels have been derived based on a theoretical relation between the depth-averaged shear stress and boundary shear stress. Equation of depth mean velocity in a rough channel is also obtained and the effects of water surface (or dip phenomenon) and roughness are included. Experimental data available in the literature have been used for verification that shows that the model reasonably agrees with the measured data.

Oscar Castro-Orgaz (2010) reanalysed the available data on turbulent velocity profiles in steep chute flow, to determine general law by taking into account both the laws of the wall and wake. Once the velocity profile is defined, an equivalent power-law velocity approximation is proposed, with generalised coefficients determined by the rational approach.

The results obtained for the turbulent velocity profiles were applied to analytically determine the resistance characteristics for chute flows.

Albayrak *et al*. (2011) combined the detailed acoustic Doppler velocity profiler (ADVP ), large-scale particle image velocimetry (LSPIV) and hot film measurements to analyse secondary current dynamics within the water column and free surface of an open channel flow over a rough movable (not moving) bed in a wider channel, with a higher bed roughness and at higher Reynolds number.

Kundu and Ghoshal (2012) re-investigated the velocity distribution in open channel flows based on flume experimental data. From the analysis, it is proposed that the wake layer in outer region may be divided into two regions, the relatively weak outer region and the relatively strong outer region. Combining the log law for inner region and the parabolic law for relatively strong outer region, an explicit equation for mean velocity distribution of steady and uniform turbulent flow through straight open channels is proposed and verified with the experimental data. It is found that the sediment concentration has significant effect on velocity distribution in the relatively weak outer region.

### 2.2.2 STRAIGHT COMPOUND CHANNELS

Wormleaton and Hadjipanos (1985) measured the velocity in each subdivision of the channel, and found that even if the errors in the calculation of the overall discharge were small, the errors in the calculated discharges in the floodplain and main channel may be very large when treated separately. They also observed that, typically, underestimating the discharge on the floodplain was compensated by overestimating it for the main channel. The failure of most subdivision methods is due to the complicated interaction between the main channel and floodplain flows.

Myers (1987) presented theoretical considerations of ratios of main channel velocity and discharge to the floodplain values in compound channel. These ratios followed a straight-

line relationship with flow depth and were independent of bed slope but dependent on channel geometry only. Equations describing these relationships for smooth compound channel geometry were presented. The findings showed that at low depths, the conventional methods always overestimated the full cross sectional carrying capacity and underestimated at large depths, while floodplain flow capacity was always underestimated at all depths. He underlined the need for methods of compound channel analysis that accurately model proportions of flow in floodplain and main channel as well as full cross-sectional discharge capacity.

Tominaga & Nezu (1992) measured velocity with a fibre-optic laser-Doppler anemometer in steep open-channel flows over smooth and incompletely rough beds. As velocity profile in steep open channel is necessary for solving the problems of soil erosion and sediment transport, and he observed the integral constant A in the log law coincided with the usual value of 5.29 regardless of the Reynolds and Froude number in subcritical flows, whereas it decreased with an increase of the bed slope in supercritical flows.

Willetts and Hardwick (1993) reported the measurement of stage–discharge relationship and observation of velocity fields in small laboratory two stage channels. It was found that the zones of interaction between the channel and floodplain flows occupied the whole or at least very large portion of the main channel. The water, which approached the channel by way of floodplain, penetrated to its full depth and there was a vigorous exchange of water between the inner channel and floodplain in and beyond the downstream half of each bend. This led to consequent circulation in the channel in the whole section. The energy dissipation mechanism of the trapezoidal section was found to be quite different from the rectangular section and they suggested for further study in this respect. They also suggested for further investigation to quantify the influence of floodplain roughness on flow parameters.

Czernuszenko, Kozioł, Rowiński (2007) describes some turbulence measurements carried out in an experimental compound channel with flood plains. The surface of the main channel bed was smooth and made of concrete, whereas the flood plains and sloping banks were covered by cement mortar composed with terrazzo. Instantaneous velocities were measured be means of a three-component acoustic Doppler velocity meter (ADV) manufactured by Sontek Inc. This article presents the results of measurements of primary velocity, the distribution of turbulent intensities, Reynolds stresses, autocorrelation functions, turbulent scales, as well as the energy spectra.

Xiaonan Tang, Donald W. Knight (2008) reviewed a model, developed by Shiono and Knight (SKM) to overcome the difficulties in defining the boundary conditions at the internal wall between the main channel and the flood plain. They proposed a novel approach for imposing the boundary conditions by taking 3sets of different experimental data.

M. M. Ahmadi *et al*. (2009) proposed an unsteady 2D depth-averaged flow model taking into consideration the dispersion stress terms to simulate the bend flow field using an orthogonal curvilinear co-ordinate system. The dispersion terms which arose from the integration of the product of the discrepancy between the mean and the actual vertical velocity distribution were included in the momentum equations in order to take into account the effect of the secondary current.

### 2.2.3 MEANDER SIMPLE CHANNELS

Johannesson and Parker (1989) presented an analytical model for calculating the lateral distribution of the depth-averaged primary flow velocity in meandering rivers. The well-known "moment method," commonly used to solve the concentration distributions, is then used to obtain an approximate solution. This makes it possible to take into account the convective transport of primary flow momentum by the secondary flow. This oft-neglected

influence of the secondary flow is shown to be an important cause of the redistribution of the primary flow velocity.

Maria and Silva (1999) expressed the friction factor of rough turbulent meandering flows as the function of sinuosity and position (which is determined by, among other factors, the local channel curvature).They validated the expression by the laboratory data for two meandering channels of different sinuosity. The expression was found to yield the computed vertically averaged flows that are in agreement with the flow pictures measured for both large and small values of sinuosity.

Zarrati, Tamai and Jin (2005) developed a depth averaged model for predicting water surface profiles for meandering channels. They applied the model to three meandering channels (two simple and one compound) data. The model was found to predict well the water surface profile and velocity distribution for simple channels and also for the main channel of compound meandering channel.

### 2.2.4 MEANDER COMPOUND CHANNEL

D. Alan Ervine, *et al*. (2000) presented a practical method to predict depth-averaged velocity and shear stress for straight and meandering overbank flows. An analytical solution to depth-integrated turbulent form of the Navier-Stokes equation was presented that included lateral shear and secondary flows in addition to bed friction. The novelty of that approach was not only its inclusion of the secondary flows in the formulation but also its applicability to straight and meandering channels.

Patra and Kar (2004) reported the test results concerning the flow and velocity distribution in meandering compound river sections. Using power law they presented equations concerning the three-dimensional variation of longitudinal, transverse, and vertical velocity in the main channel and floodplain of meandering compound sections in terms of channel parameters. The results of formulations compared well with their respective

experimental channel data obtained from a series of symmetrical and unsymmetrical test channels with smooth and rough surfaces. They also verified the formulations against the natural river and other meandering compound channel data.

## 3.0 OVERVIEW OF NUMERICAL MODELLING ON OPEN CHANNEL FLOW

For the past three decades, flow in simple and compound meandering channels has been extensively studied both experimentally and numerically. Various numerical models such as standard k-ε model, non-linear k-ε model, k-ω model, algebraic Reynolds stress model (ASM), Reynolds stress model (RSM) and large eddy simulation (LES) have been developed to simulate the complex secondary structure in compound meandering channel. The standard k- ε model is an isotropic turbulence closure but fails to reproduce the secondary flows. Although nonlinear k- ε model can simulate secondary currents successfully in a compound channel, it cannot accurately capture some of the turbulence structures. ASM is economical because it uses adhoc expressions to solve Reynolds stress transport equations. But the simulated results by ASM found to be unreliable. Reynolds stress model (RSM) computes Reynolds stresses by directly solving Reynolds stress transport equation but its application to open channel is still limited due to the complexity of the model. Large eddy simulation (LES) solves spatially-averaged Navier-Stokes equation. Large eddies are directly resolves, but the eddies smaller than mesh are modelled. LES is computationally very expensive to be used for industrial application.

Giuseppe Pezzinga (1994) examined the problem of prediction of uniform turbulent flow in a compound channel with the nonlinear k-ε model. This model is capable of predicting the secondary currents, caused by the anisotropy of normal turbulent stresses that are important features of the flow in compound channels, as they determine the transverse momentum transfer. The comparison shows that the model predicts with accuracy the

distribution of the primary velocity component, the secondary circulation, and the discharge distribution. The numerical results are used to search a subdivision surface between main channel and floodplain on the basis of the flow field and to compare different subdivision surfaces on the basis of the discharge distribution by a simple uniform flow formula, The better subdivision surfaces as predicted by the model are the diagonal surface going from the corner between main channel and floodplain to the free surface on the symmetry plane and the bisector of the same corner.

Cokljat and Younis and Basara and Cokljat (1995) proposed the RSM for numerical simulations of free surface flows in a rectangular channel and in a compound channel and found good agreement between predicted and measured data.

Thomas and Williams (1995) describes a Large Eddy Simulation of steady uniform flow in a symmetric compound channel of trapezoidal cross-section with flood plains at a Reynolds number of 430,000. The simulation captures the complex interaction between the main channel and the flood plains and predicts the bed stress distribution, velocity distribution, and the secondary circulation across the floodplain. The results are compared with experimental data from the SERC Flood Channel Facility at Hydraulics Research Ltd, Wallingford, England.

Salvetti et al. (1997) has conducted LES simulation at a relatively large Reynolds number for producing results of bed shear, secondary motion and vorticity well comparable to experimental results.

Rameshwaran P, Naden PS.(2003) analyzed three dimensional nature of flow in compound channels.

Sugiyama H, Hitomi D, Saito T.(2006) used turbulence model consists of transport equations for turbulent energy and dissipation, in conjunction with an algebraic stress model

based on the Reynolds stress transport equations. They have shown that the fluctuating vertical velocity approaches zero near the free surface. In addition, the compound meandering open channel is clarified somewhat based on the calculated results. As a result of the analysis, the present algebraic Reynolds stress model is shown to be able to reasonably predict the turbulent flow in a compound meandering open channel.

Kang H, Choi SU. (2006) used a Reynolds stress model for the numerical simulation of uniform 3D turbulent open-channel flows. The developed model is applied to a flow at a Reynolds number of 77000 in a rectangular channel with a width to depth ratio of 2. The simulated mean flow and turbulence structures are compared with measured and computed data from the literature. It is found that both production terms by anisotropy of Reynolds normal stress and by Reynolds shear stress contribute to the generation of secondary currents.

Jing, Guo and Zhang (2008) simulated a three-dimensional (3D) Reynolds stress model (RSM) for compound meandering channel flows. The velocity fields, wall shear stresses, and Reynolds stresses are calculated for a range of input conditions. Good agreement between the simulated results and measurements indicates that RSM can successfully predict the complicated flow phenomenon.

Cater and Williams (2008) reported a detailed Large Eddy Simulation of turbulent flow in a long compound open channel with one floodplain. The Reynolds number is approximately 42,000 and the free surface was treated as fully deformable. The results are in agreement with experimental measurements and support the use of high spatial resolution and a large box length in contrast with a previous simulation of the same geometry. A secondary flow is identified at the internal corner that persists and increases the bed stress on the floodplain.

Kim et al. (2008) analyses three-dimensional flow and transport characteristics in two representative multi-chamber ozone contactor models with different chamber width using LES.

Wang *et.al*., (2008) used different turbulence closure schemes i.e., the mixing-length model and the *k-ε* model with different pressure solution techniques i.e., hydrostatic assumptions and dynamic pressure treatments are applied to study the helical secondary flows in an experiment curved channel. The agreements of vertically-averaged velocities between the simulated results obtained by using different turbulence models with different pressure solution techniques and the measured data are satisfactory. Their discrepancies with respect to surface elevations, super elevations and secondary flow patterns are discussed.

Balen et.al. (2010) performed LES for a curved open-channel flow over topography. It was found that, notwithstanding the coarse method of representing the dune forms, the qualitative agreement of the experimental results and the LES results is rather good. Moreover, it is found that in the bend the structure of the Reynolds stress tensor shows a tendency toward isotropy which enhances the performance of isotropic eddy viscosity closure models of turbulence.

Beaman (2010) studied the conveyance estimation using LES method.

Esteve *et.al.,* (2010) simulated the turbulent flow structures in a compound meandering channel by Large Eddy Simulations (LES) using the experimental configuration of Muto and Shiono (1998). The Large Eddy Simulation is performed with the in-house code LESOCC2. The predicted stream wise velocities and secondary current vectors as well as turbulent intensity are in good agreement with the LDA measurements.

Larocque, Imran, Chaudhry (2013) presented 3D numerical simulation of a dam-break flow using LES and k- ε turbulence model with tracking of free surface by volume-of-fluid model. Results are compared with published experimental data on dam-break flow through a

partial breach as well as with results obtained by others using a shallow water model. The results show that both the LES and the k –ε modelling satisfactorily reproduce the temporal variation of the measured bottom pressure. However, the LES model captures better the free surface and velocity variation with time.

# EXPERIMENTAL WORK AND METHODOLOGY

## 3.1 OVERVIEW

Evaluation of discharge capacity in a meandering river channels is a complicated process due to variations in geometry, surface roughness, channel alignments and flow conditions. The evaluation of discharge capacity is directly dependent on accurate prediction of knowledge of velocity distribution in channel. Velocity distribution is never uniform across a compound channel cross-section. It is higher in deeper main channel than the shallower floodplain, as in compound channels the shallow floodplains offer more resistance to flow than the deep main channel. Variation of velocity leads to lateral momentum transfer between the deep main channel and the adjoining shallow floodplains. This further complicates the flow process, leading to the uneven distribution of shear stress in the main channel and floodplain peripheral regions. The trends and behaviour pattern observed in the laboratory flumes can be used in better understanding of the mechanism of flow in a meandering channel and so for the solution of many practical river problems.

In the present work the velocity distribution has been studied through a series experimental runs in a meandering channel of higher sinuosity existing in the laboratory. Details of hydraulics and geometric parameters of meandering channel, apparatus and measuring equipments used and working procedure adopted has been outlined in this chapter.

## 3.2 APPARATUS & EQUIPMENTS USED

In this study Measuring devices like a pointer gauge having least count of 0.1 mm, rectangular notch, five micro-Pitot tubes each of them having 4.6 mm external diameter and five manometers were used in the experimentation. These are used to measure velocity and its direction of flow in the channels. Including these also useful apparatus without which

experiments could not be possible. Those were baffle walls, stilling chamber, baffle, head gate, travelling bridge, sump, tail gate, volumetric tank, over head tank arrangement, water supply devices, two parallel pumps etc. The measuring equipments and the devices were arranged properly to carry out experiments in the channels. Keeping the set up with sufficient care and management experiments runs were taken for the meandering channel.

### 3.3 EXPERIMENTAL SETUP AND PROCEDURE

Experiments are conducted utilising the channel facility available at the Hydraulics Laboratory of the Civil Engineering Department, National Institute of Technology, Rourkela. The experimental meandering channel is fabricated using 6mm thick Perspex sheet inside a tilting flume. The tilting flume is 15m long having a rectangular cross-section of 4m wide and 0.5m deep, made up of deep metal frame with glass walls. The flume can be tilted to different bed slopes by hydraulic jack arrangement. The experimental meandering channel has trapezoidal cross-section. All observations are recorded at the central bend apex. Photograph of the experimental meandering channel with measuring equipments are shown in Photo.3.1 (a, b). Fig.3.2 (a, b) shows the plan view of half meander wavelength with dimensional details while the plan view of full length experimental channel with other arrangements is shown in Fig.3.1.

Experimental channel**:** The meandering channel is trapezoidal in cross section. The channel is 330 mm wide at bottom, 460 mm at top having full depth of 65 mm, and side slopes of 1:1. The channel has wavelength $L$ = 3972 mm and double amplitude $2A'$ = 1365 mm. Sinuosity for this channel is scaled as 2.04 Photo. 3.1(a, b). For better information, the geometrical parameters and hydraulic details of the experimental runs of the channel is tabulated below.

**Channel Photographs**

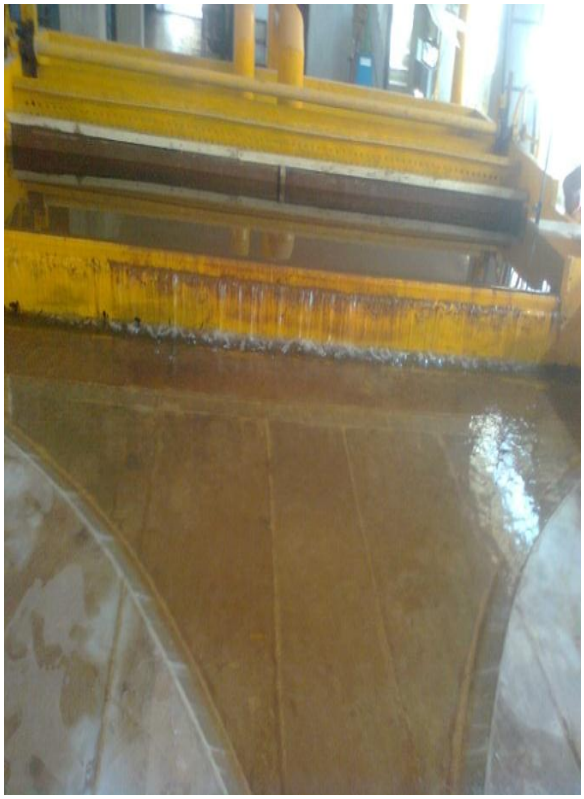

**Photo.3.1 (a) View of Experimental Channel** **Photo.3.1 (b) Rectangular Notch**

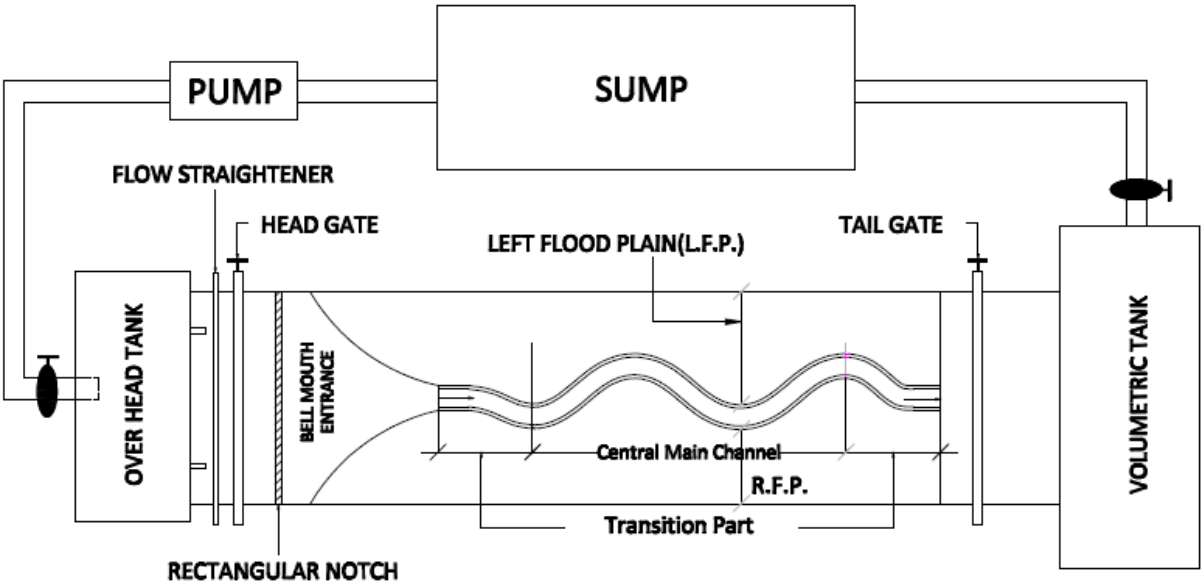


**Fig.3.1 *Schematic diagram of Experimental Setup**

*****After Mohanty et.al (2013)*

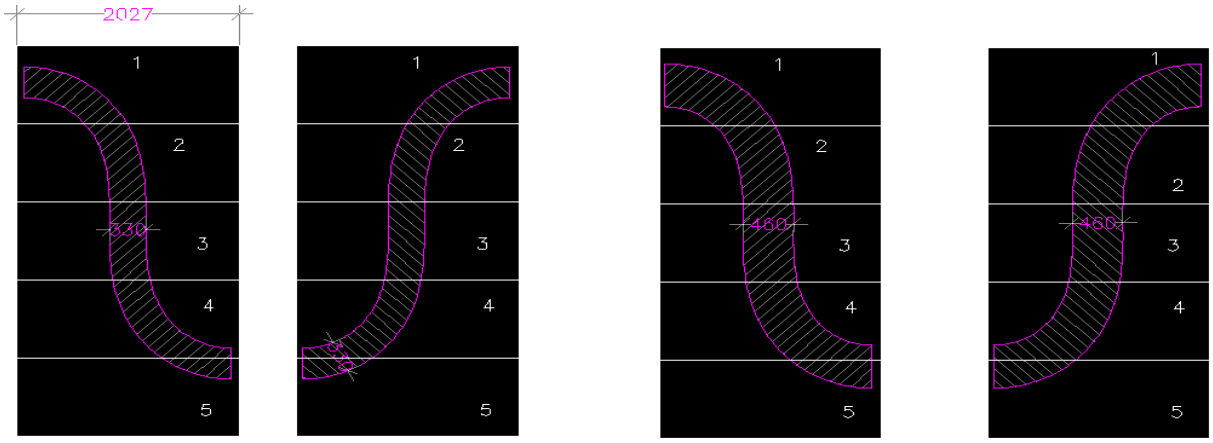


**3.2(a) At Bed Level** **3.2(b) At 6.5cm above Bed**

**Fig. (3.2) Sectional Plan View**

**Table 1. Geometry Parameters of the Experimental Meandering Channel**

| Sl. No. | Item Description | Highly Meander channel |
|---|---|---|
| 1. | Wave length in down valley direction | 4054 mm |
| 2. | Amplitude | 2027 mm |
| 3. | Geometry of main channel section | Trapezoidal (side slope 1:1) |
| 4. | Main channel width ($b$) | 330mm at bottom |
| 5. | Bank full depth of main channel | 65mm |
| 6. | Top width of main channel ($B$) | 460 mm |
| 7. | Slope of the channel | 0.0055 |
| 8. | Meander belt width ($B_W$) | 2357 mm |
| 9. | Nature of surface bed | Smooth and rigid bed |
| 10. | Sinuosity($S_r$) | 2.04 |
| 11. | Cross over angle in degree | 90° |
| 12. | Flume size | 15m*4m*0.5m |

A numbers of parallel pumps are used to pump water at the rate up to 200 lit/sec from an underground sump to the overhead tank. From the over head tank, water is led to a stilling tank located at the upstream of the channel. A series of baffle walls are provided between the stilling tank and channels to reduce turbulence of the incoming water. From the stilling tank water is allowed to flow through the meandering channel under gravity. Towards the end of the experimental channel, water is allowed to flow through a tilting type tailgate and is collected in a masonry volumetric tank from where it is again flow back to the underground sump. From the sump, water is then pumped back to the overhead tank, thus setting a

complete re-circulating system of water supply for the experimental channel. Here the role of tailgate is to maintain the uniform flow in the channel. Each experimental runs of the channel are carried out by maintaining the water surface slope parallel to the valley slope to achieve the steady and uniform flow conditions. In all the experimental runs this simplified approach has been tried to achieve which is also in line with the experimental work of Shino, Al-Romaih and Knight (1999). This stage of flow is considered as normal depth, which can carry a particular flow only under steady and uniform conditions.

At the top of the experimental flume, main guide rails are provided on which a travelling bridge is moved in the longitudinal direction of the entire experimental channel. The point gauge and a micro-Pitot tube of 4.6 mm external diameter are attached to the travelling bridge with secondary guide rails allowing the equipments to move in both longitudinal and the transverse direction of the experimental channel. Water surface slope measurement is carried out using a pointer gauge fitted to the travelling bridge. It is having least count of 0.1 mm and operated manually. There are five Pitot tubes that are in conjunction with suitable five manometers are used to measure point velocity and its direction of flow at the predefined points of the flow-grid. The Pitot tube is physically rotated normal to the main stream direction till it gives maximum deflection of manometer reading. The angle of limb of Pitot tube with longitudinal direction of the channel is noted by the circular scale and pointer arrangements attached to the flow direction meter. A rectangular notch has also been fabricated and placed at the u/s face which is calibrated to find the continuous stage-discharge relationships of the channels. Observations are recorded for different flow depths, only under steady and uniform conditions.

### 3.3.1 Measurement of Bed Slope

The impounded water in the channel is kept still by blocking the tail gate provided towards the end of experimental channel. Then bed and water surface level are recorded using a pointer gauge having least count 0.1 mm from the standing water at a certain point. This procedure is repeated again and observations are recorded at a distance of one wavelength along its centreline. The mean slope for the meandering channels is obtained by dividing the level difference of channel bed and water surface between these two points by the length of meander wave along the centreline.

### 3.3.2 Calibration of Notch

For accurate discharge estimation a rectangular notch is fitted at the upstream side of the flume. It required calibration before measuring the discharge. For this, area of volumetric tank located at the end of channel to receive the incoming water flow through the channels is measured properly. The height of water in the volumetric tank collected from channel is recorded form the water level measuring scale connected to it. Then time is recorded using a stopwatch with respect to the collection of water in that tank. Time variation depends on the rate of flow from the channel. Finally change in the mean water level in the tank over the time interval is recorded. From the knowledge of the volume of water collected in the measuring tank and the corresponding time of collection, the actual discharge flowing in the experimental channel for each run of each channel is obtained. The height of water flowing above the rectangular notch is measured by point gauge attached to the notch. Then form calibration the coefficient of discharge '$C_d$'for each run is calculated as for the equation given below.

$$Q_a = C_d Q_t$$

$$Q_a = Ah_v$$

$$Q_t = \frac{2}{3} L\sqrt{2g} H_n^{2/3}$$

Where

$Q_a$ = Actual discharge

$Q_t$ = Theoretical discharge

$A$ = Area of volumetric tank

$C_d$ = Coefficient of discharge calculated from notch calibration

$h_w$ = Height of water in the volumetric tank

$L$ = Length of the notch

$H_n$ = Height of water above the notch

$g$ = Acceleration due to gravity

From the notch calibration coefficient of discharge '$C_d$' for rectangular notch is found to be **0.71**.

### 3.3.3 Measurement of Depth of flow and Discharge

Depth of flow for all the series of experimentation is measured by point gauge above the bed of the channel. The point gauge with least count of 0.1 mm is fitted to the travelling bridge and operated manually. A rectangular notch has also been fabricated for the purpose of discharge estimation and placed at the u/s face which is calibrated to find the continuous discharge measurement of channels. A volumetric tank located at the end of channel to receive the incoming water flow through the channels. The discharge '$Q_a$'for each run is

calculated as for the equation given below.

$$Q_a = C_d \frac{2}{3} L\sqrt{2g} H_n^{2/3}$$

Where

$Q_a$ = Actual discharge

$C_d$ = Coefficient of discharge calculated from notch calibration

$L$ = Length of the notch

$H_n$ = Height of water above the notch

$g$ = Acceleration due to gravity

### 3.3.4 Measurement of tangential Velocity

Velocity measurements are taken at the bend apex in meandering channel due to minimum curvature effect and to study the flow parameters covering half the meander wave length. In the present work velocity readings are taken using Pitot tubes. These are placed in the direction of flow and then allowed to rotate along a plane parallel to the bed and till a relatively maximum head difference appeared in manometers attached to the respective Pitot tubes. The deviation angle between the reference axis and the total velocity vector is assumed to be positive, when the velocity vector is directed away from the outer bank. The total head *h* reading by the Pitot tube at the predefined points of the flow-grid in the channel is used to measure the magnitude of point velocity vector as $U = (2gh)^{1/2}$, where *g* is the acceleration due to gravity. Resolving *U* into the tangential and radial directions, the local velocity components is obtained. Here the tube coefficient is taken as unit and the error due to turbulence considered negligible while measuring velocity. Point velocities were measured along verticals spread across the main channel and flood plain so as to cover the width of

entire cross section. Also at a no. of horizontal layers in each vertical, point velocities were taken. Particularly the point velocities at a depth of 0.4H (where H is the depth of flow at that lateral section across the channel) from channel bed in main channel region and 0.4(H-h) on floodplains (h is depth of main channel) were measured throughout the lateral section of the compound cross section to experimentally determine the depth averaged velocity distribution under each discharge condition. Measurements were thus taken from left edge point of flood plain to the right edge of floodplain including the main channel bed and side slope (Figure.3.3 (a, b) shows the grid diagram used for experiments). Velocity measurements were taken by five pitot static tube (outside diameter 4.77mm) connected with five piezometers fitted inside a transparent fiber block fixed to a wooden board and hung vertically at the edge of flume the ends of which were open to atmosphere at one end and connected to total pressure hole and static hole of pitot tube by long transparent PVC tubes at other ends. Before taking the readings the pitot tube along with the long tubes measuring about 5m were to be properly immersed in water and caution was exercised for complete expulsion of any air bubble present inside the pitot tube or the PVC tube. Even the presence of a small air bubble inside the static limb or total pressure limb could give erroneous readings in piezometers used for recording the pressure.

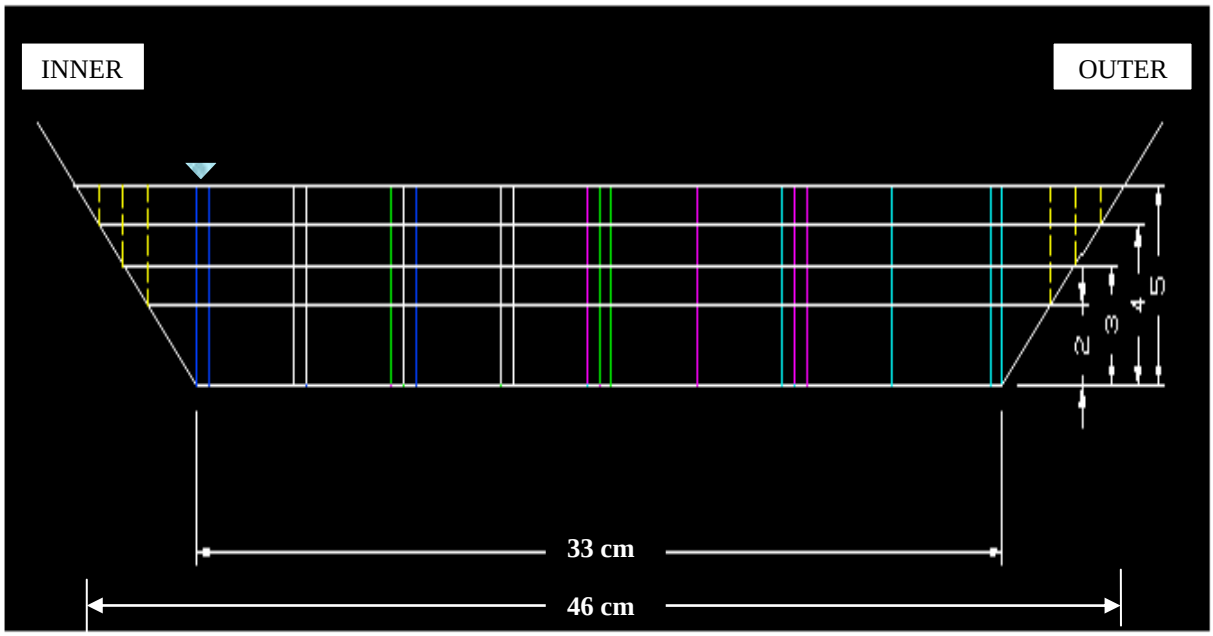


**(a) Meander simple cross section**

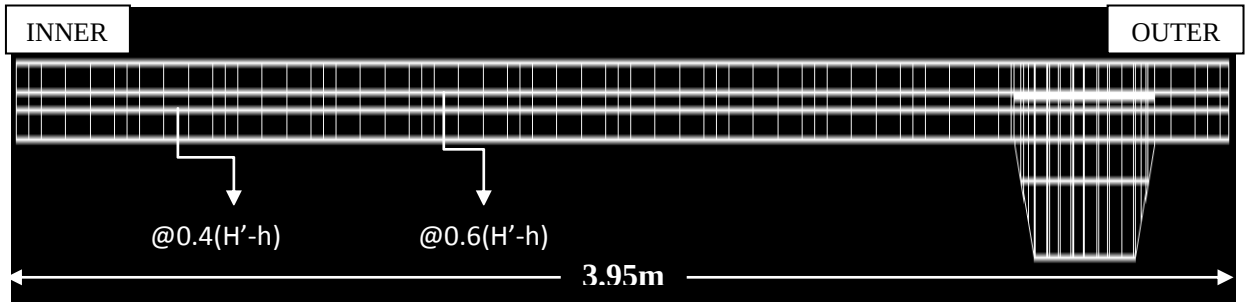


**(b) Meander compound channel cross section**

**Fig. (3.3) Meander channel cross section with the grid of measurement points for velocity**

Each experimental runs of the channel are carried out by maintaining the water surface slope parallel to the valley slope to achieve the steady and uniform flow conditions. In Stage-discharge relationships are found out for meandering channels having rigid and smooth boundaries.

## 4.1 OVERVIEW

The results of experiments concerning the distribution of velocity, flow in the meandering channels are presented in this chapter. Analysis is also done for depth averaged velocity in the meandering channel. The overall summary of experimental runs for the meandering channel is given in Table-2.

## 4.2 STAGE-DISCHARGE RELATIONSHIP IN MEANDERING CHANNELS

In the present work it was not easy to achieve steady and uniform flow condition in meandering channels due to the effect of curvature and the influence of a number of geometrical and hydraulic parameters. However, it is tried to achieve the water surface slope parallel to the valley slope so as to get an overall steady and uniform flow in the experimental channels. In all the experimental runs this simplified approach has been tried to achieve which is also in line with the experimental work of Shino, Al-Romaih and Knight (1999). This stage of flow is considered as normal depth, which can carry a particular flow only steady and uniform condition. The stage discharge curves plotted for meandering channel of sinuosity 2.04 is shown in Fig. 4.1. From the figure it is seen that the discharge increases with an increase in stage in the channel.

**Table 2. Hydraulic parameters for the experimental runs**

| Runs | Discharge Q (in lit/s) | Flow depth H (in cm) | Relative depth β | Froude No. ($F_r$) | Reynolds No. (R) |
|---|---|---|---|---|---|
| ***INBANK FLOW*** | | | **(H/h)** | | |
| 1 | 1.165 | 1.7 | 0.2615 | 0.495 | 3847.90 |
| 2 | 1.872 | 2.5 | 0.3846 | 0.441 | 5832.49 |
| 3 | 3.803 | 3.8 | 0.5846 | 0.468 | 10851.62 |
| 4 | 4.153 | 4.0 | 0.6154 | 0.471 | 11701.64 |
| 5 | 6.055 | 5.0 | 0.7692 | 0.484 | 16035.97 |
| 6 | 7.5 | 5.8 | 0.8923 | 0.473 | 18953.12 |
| ***OVERBANK FLOW*** | | | **(H'-h /H')** | | |
| 1 | 18.564 | 8.9 | 0.2697 | 0.314314 | 28389.52 |
| 2 | 33.227 | 9.5 | 0.3158 | 0.397014 | 39091.89 |
| 3 | 42.513 | 9.9 | 0.3434 | 0.464403 | 46843.45 |
| 4 | 46.635 | 10.1 | 0.3564 | 0.495639 | 53654.54 |
| 5 | 52.533 | 10.6 | 0.3868 | 0.521894 | 629621.90 |

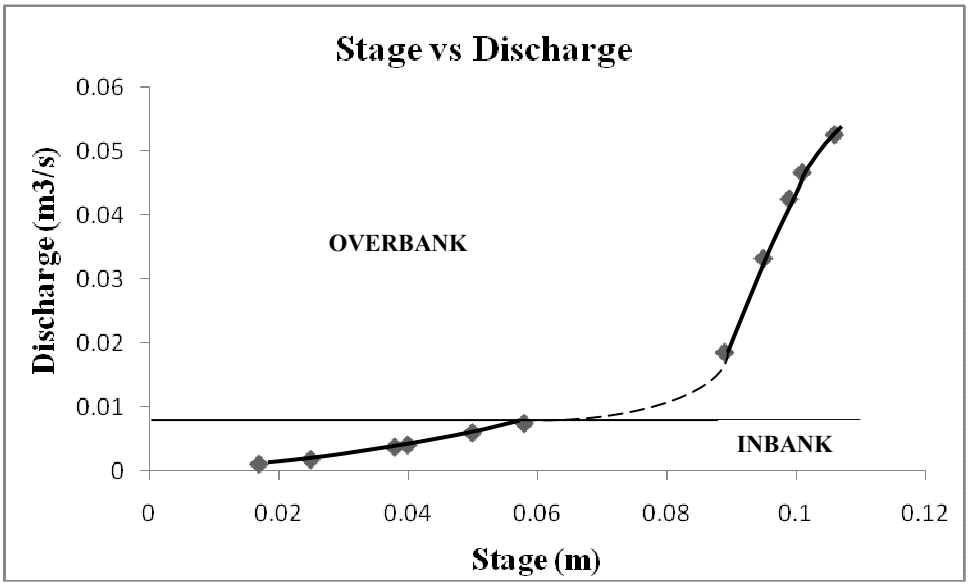


**Fig.4.1 Stage vs Discharge graph**

## 4.3 DISTRIBUTION OF LONGITUDINAL VELOCITY

Longitudinal velocity is recorded by pitot-tube in the experimental meandering channels. In these channels, observations are recorded at the bend apex with a direction normal to flow direction. The detailed velocity distribution is carried out for meandering channel of sinuosity

**2.04**. The radial distribution of longitudinal velocity in contour form for the runs of the meandering channel is shown below. It gives the point form velocity measurement at that depth of flow. The radial distribution of tangential velocity for four flow inbank depths are shown in Figs.4.2 (a, b, c and d) and for four overbank flow depths in Figs.4.3 (a,b,c,d).

### 4.3.1 INBANK VELOCITY CONTOURS

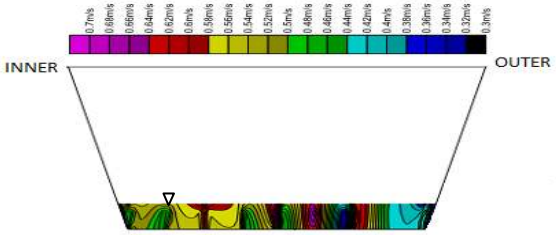


**Fig.4.2 (a) Flow Depth (*h*) = 1.7 cm**

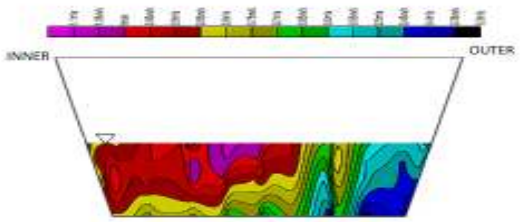


**Fig. 4.2(b) Flow Depth (*h*) = 3.8 cm**

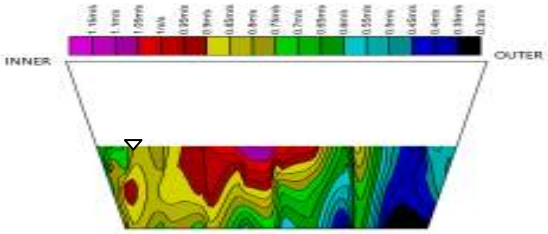


**Fig.4.2(c) Flow Depth (*h*) = 4 cm**

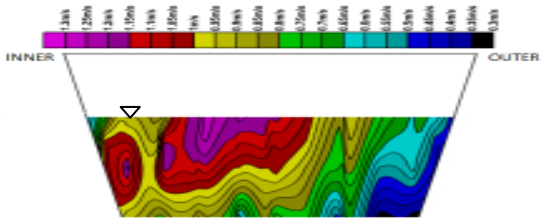


**Fig. 4.2(d) Flow Depth (*h*) = 5 cm**

**Fig.4.2 Velocity contours for different inbank depths**

From the above velocity contours, the following inferences can be drawn:

I. The location of thread of maximum longitudinal velocity prevails near the free surface. The magnitude of velocity is quite higher near inner wall than that of the outer wall.

II. The thread of lower values of velocity occurs near the outer region and these values go on increasing with increase in flow depth.

III. The concentrations of average velocity are remarkably more shifted towards the inner region than outer region.

## 4.3.2 OVERBANK VELOCITY CONTOURS

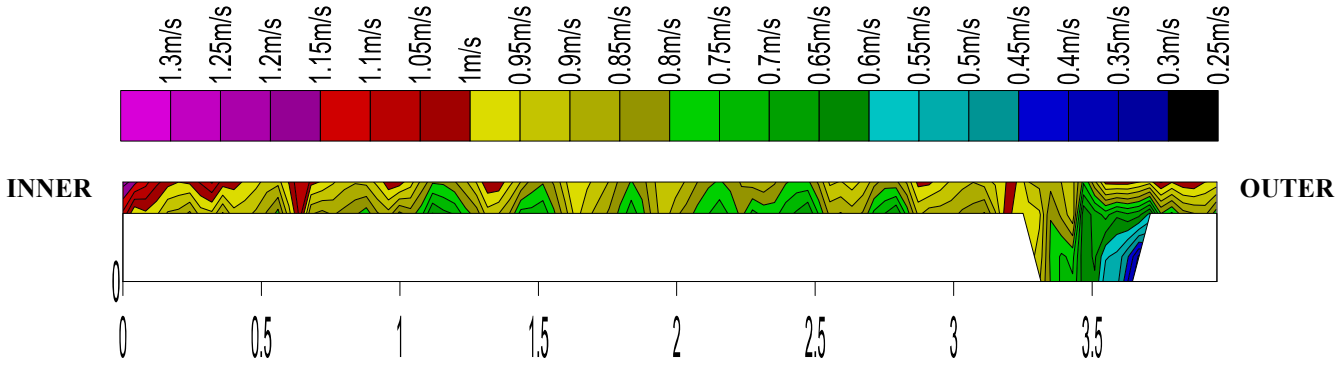


**Fig.4.3 (a) Flow Depth (H'-*h*) = 3.0 cm**

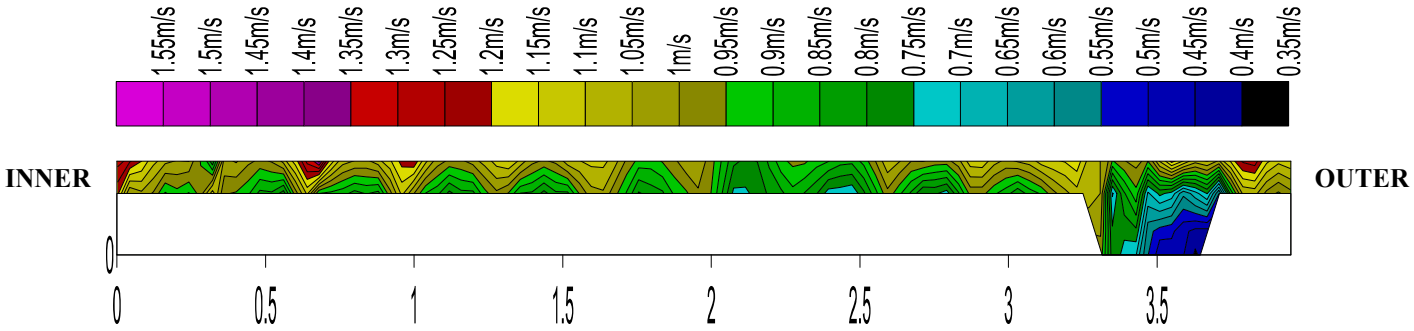


**Fig.4.3 (b) Flow Depth (H'-*h*) = 3.4 cm**

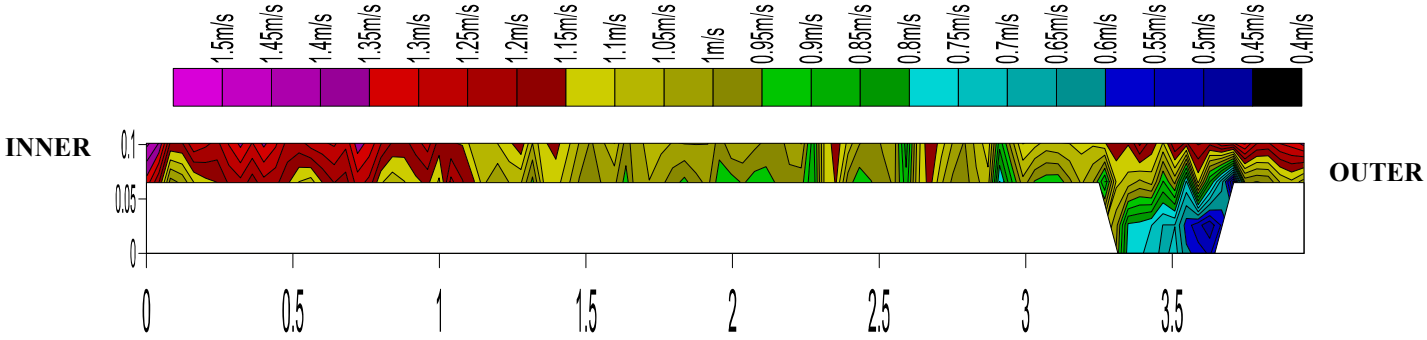


**Fig.4.3 (c) Flow Depth (H'-*h*) = 3.6 cm**

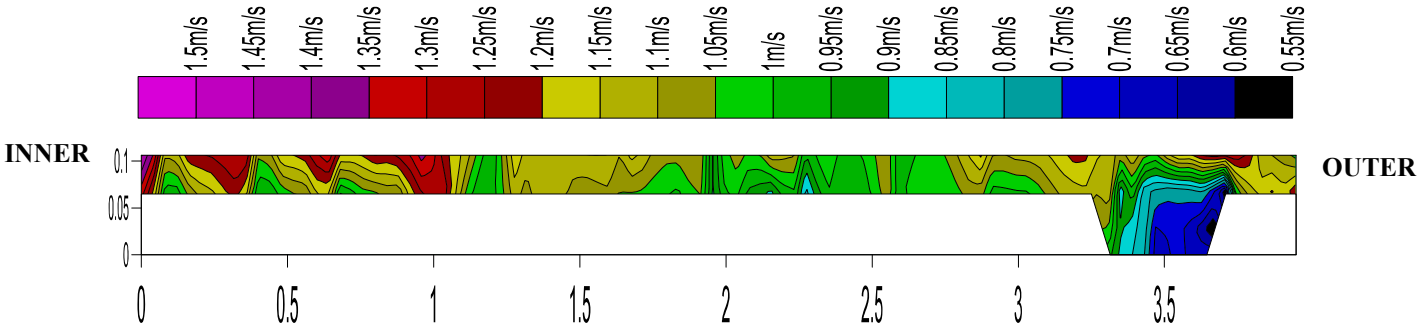


**Fig.4.3 (d) Flow Depth (H'-*h*) = 4.1 cm**

**Fig.4.3 Velocity contours for different overbank depths**

From the isovels of longitudinal velocity (Fig. 4.3 (a) to Fig. 4.3 (d)) for the meander channel -floodplain geometry, the following features are noted.

I. Interestingly it is found that the sequence of overbank isovels somewhat coincides with inbank velocity isovels.

II. The lowest velocity contour lines are found to occur at outer main channel bottom corner and its concentration increases with the increase in flow depth over the flood plain.

III. The maximum value of stream wise velocity lies near the free surface and towards the inner flood plain.

IV. The mean velocity exists mostly in the left flood plain region.

V. The occurrence of higher velocity values are more in inner flood plain region than that of outer flood plain region.

## 5.1 OVERVIEW

Once normal depth conditions were established for a given discharge, point velocity measurements were made across one section of the channel at z = 0.4h from the bed. At each lateral position, a number of readings were taken at constant intervals and then averaged to reduce error.

## 5.2 LATERAL DISTRIBUTION OF DEPTH AVERAGED VELOCITY

### 5.2.1 Inbank Flow Studies

The lateral variation of depth averaged velocity along the channel bed and wall for different inbank depths, observed at 0.4 times the depth of flow is shown in Figs.5.1. Series 1 depicts the observed values of lateral distribution of depth-averaged velocity for experimental meandering channels while Series 2 shows the cross-section of trapezoidal meandering channel at the bend apex.

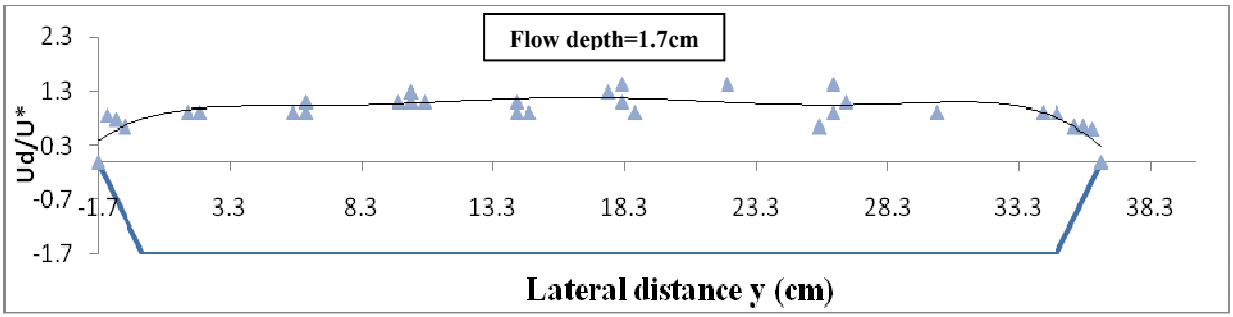


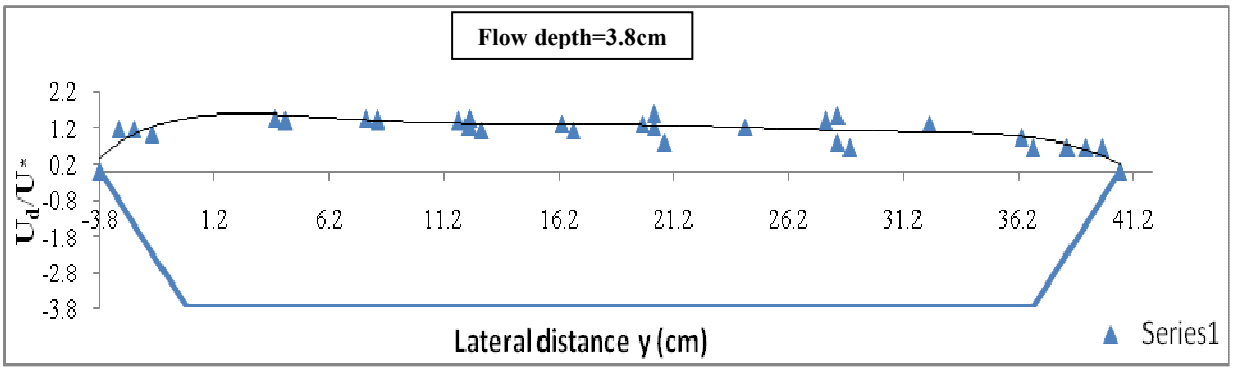

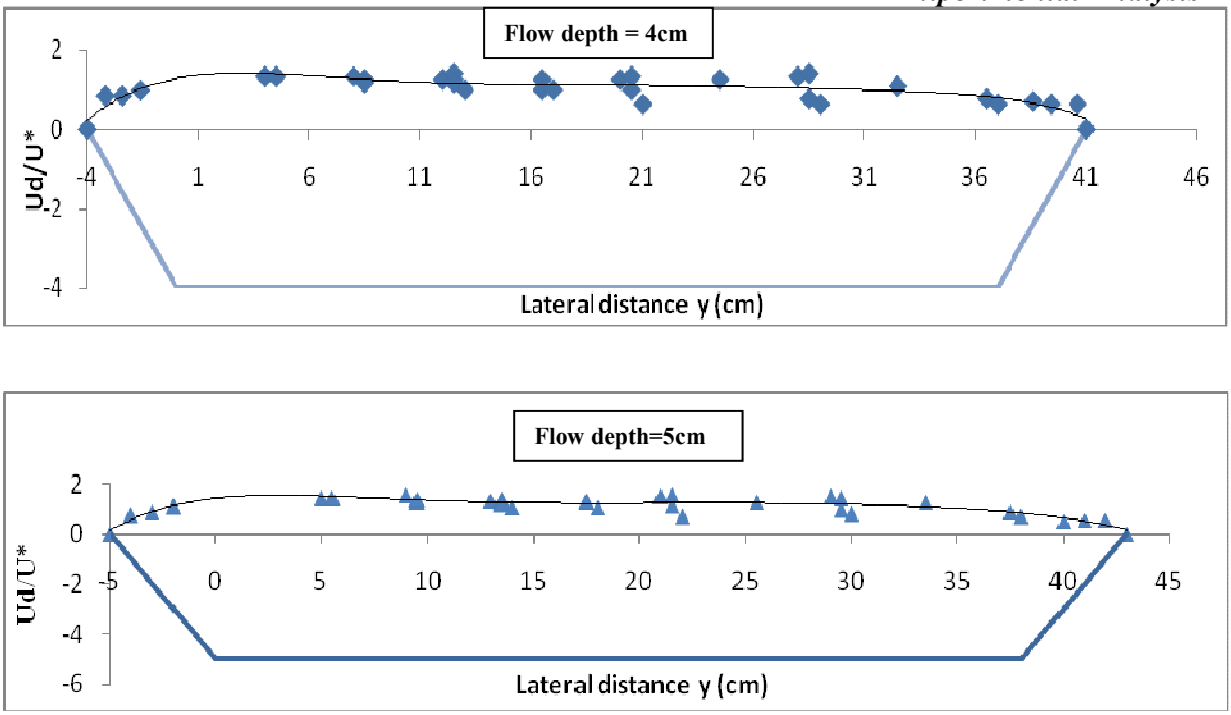


**Fig.5.1 Lateral Distribution of Normalised Depth-Averaged Velocity along the cross-section of Experimental Channel at Bend Apex for different inbank depths**

Normalised depth-averaged velocities ($U_d/U^*$) at the inner wall are found to be higher than the outer wall in the meandering channel contrary to straight channels (Wilkerson *et.al.*, 2005).

Plots of depth averaged velocity distribution versus the distance in the lateral direction are shown in Fig. 5.2. It can be seen from the figure that the depth averaged velocity is maximum around the centre line of the channel axis at the bend apex.

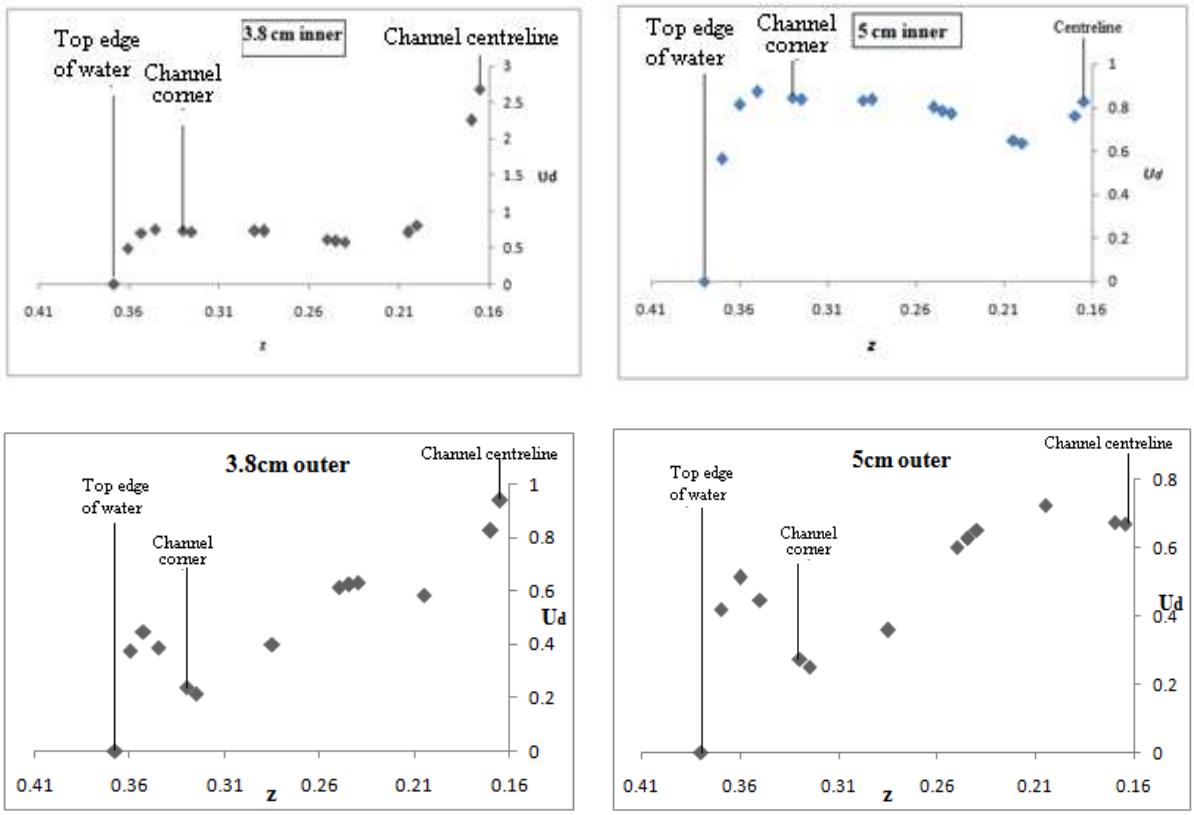


**Fig.5.2 Plot of Lateral Depth-averaged velocity distribution vs Lateral distance**

The depth averaged velocity is found to be maximum (Fig. 5.2) along the centre line axis of meander channel at the bend apex. This is in line with the observations for natural straight and curved channels. As one move from centre line towards the channel corner, decrease in the depth average velocity is marked and the maximum decrease is observed at the region of nearly 25% of radial distance from the centre line of meander channel, both in the inner and outer directions. The rate of decrease is faster for lower depths of flow than for higher depths.

### 5.2.2 Overbank Flow Studies

The lateral variation of depth averaged velocity along the channel bed and wall for different floodplain depths, observed at 0.4 times the depth of flow and is validated with CES data points, is shown in Figs.5.3. Series 1 depicts the experimental depth average values while Series 2 shows the yielded values of depth average velocity by a 1D modelling software CES.

Overbank flow cases are complicated processes to model due to the presence of turbulent structures ranging from large to small scales which transfers momentum from faster moving fluids in main channel to relatively slower fluid in flood plain while increasing and decreasing the conveyance respectively. Therefore a lot of experimental and numerical approaches has been recently adopted to quantify this lateral momentum transfer at the main channel and flood plain interface. This accretion in technical knowledge compel operating authorities should use recent improved knowledge on conveyance to reduce uncertainty in flood predictions. Taking this into account a team of experts led by HR Wallingford introduced a new Conveyance Estimation System (CES) which is being adopted in England, Wales, Scotland and Northern Ireland. CES has been recommended for use in natural rivers, artificial straight and meandering channels for estimating conveyance, computing stage discharge relationship and also a number of flow parameters like depth averaged velocity, boundary shear, shear velocity, energy coefficients etc. The software includes a roughness advisor, conveyance generator, and an uncertainty estimator. The conveyance generator is based on 1D Shiono and Knight Conveyance estimation method (SKM). Previously conveyance estimation methods incorporate only roughness parameter such as Manning's $n$, Chezy's $C$ and Darcy Weisbach $f$, but SKM consists three calibration constants: Weisbach $f$, dimensionless eddy viscosity $\lambda$, transverse gradient of secondary flow term $\Gamma$. Therefore it precisely models the flow to reduce uncertainties in the estimation of river flood levels, discharge and velocities.

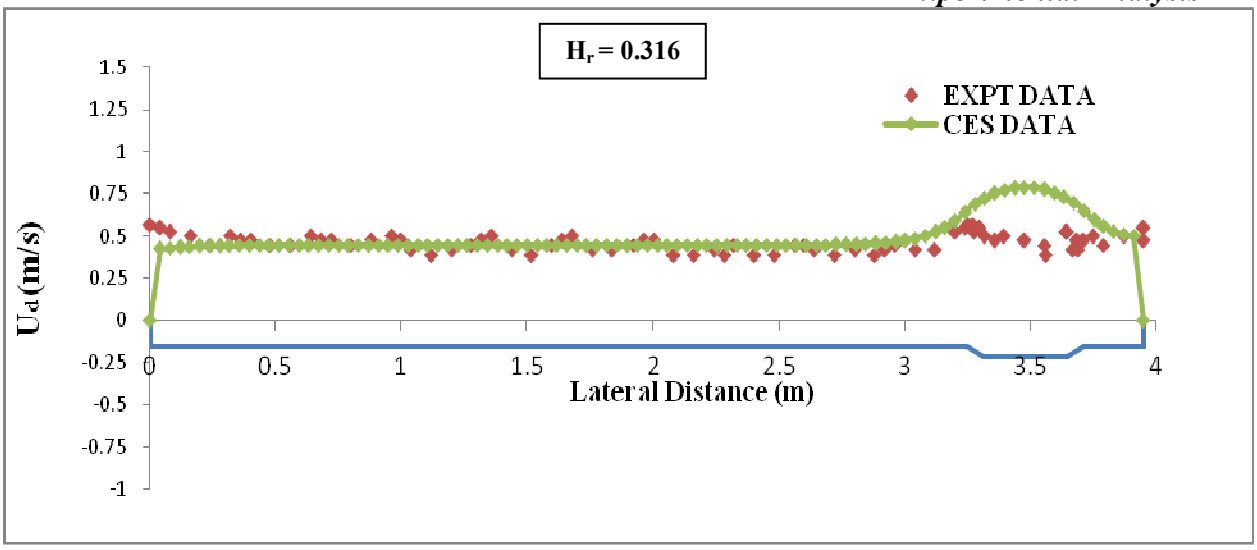
$H_r$ = 0.316
EXPT DATA
CES DATA
$U_d$ (m/s)
Lateral Distance (m)

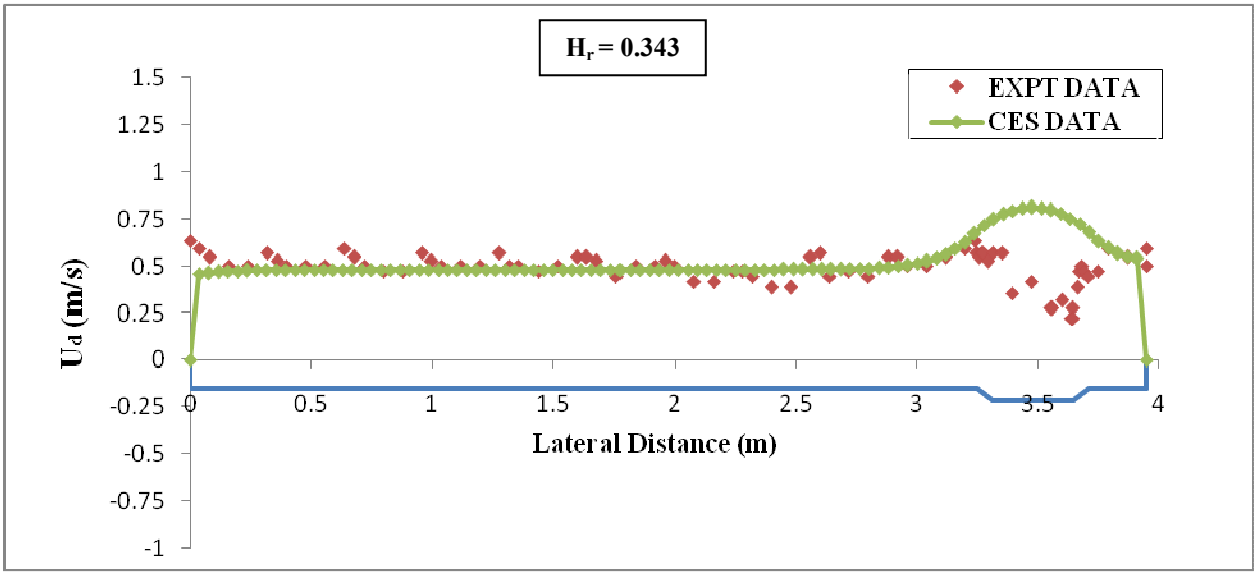
$H_r$ = 0.343
EXPT DATA
CES DATA
$U_d$ (m/s)
Lateral Distance (m)

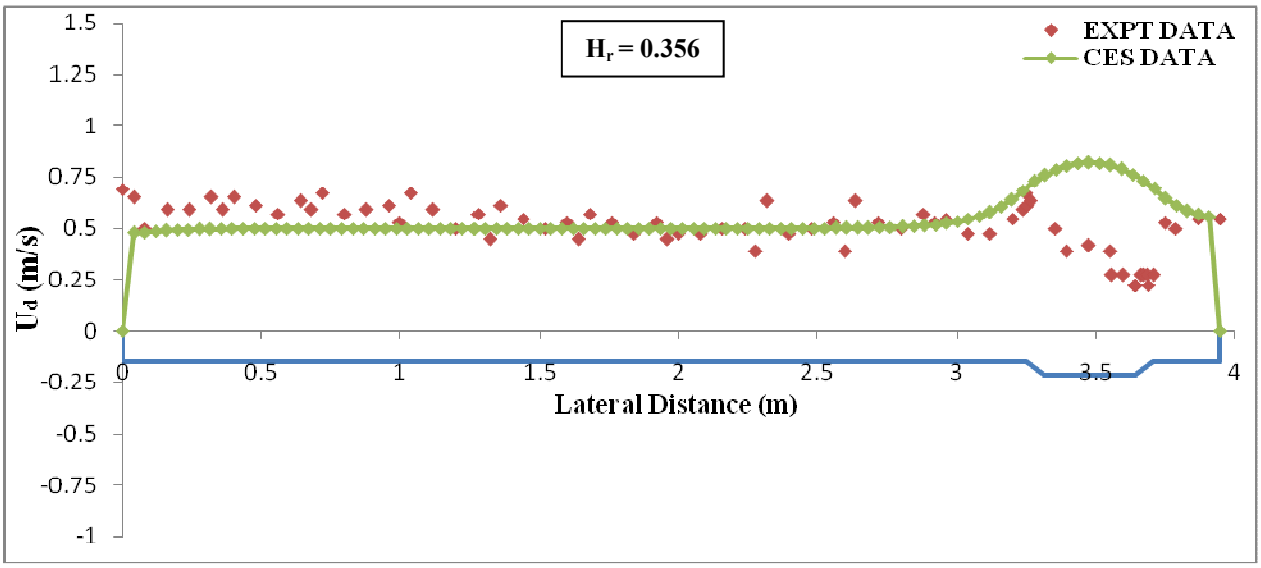
$H_r$ = 0.356
EXPT DATA
CES DATA
$U_d$ (m/s)
Lateral Distance (m)

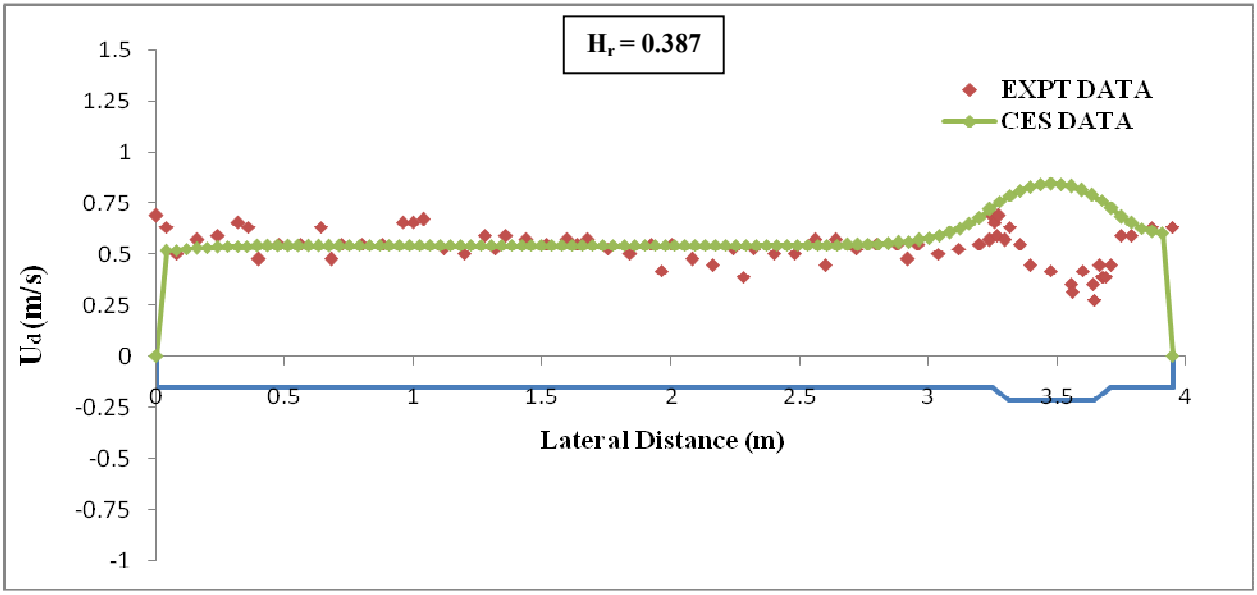


**Fig.5.3 Lateral Distribution of Depth-Averaged Velocity along the compound cross-section of Experimental Channel at Bend Apex for different relative depths**

It can be observed from the Figs. 5.3 that the higher values of depth averaged velocity are found at the inner flood plain region and attain a maximum value at the junction between the main channel bank and the flood plain. It can also be seen that the minimum depth average velocity values occurred at the junctions between the bed and the outer bank of main channel.

Wilkerson *et al*., (2005) proposed two models to fit data from three independent studies for straight trapezoidal channels. The second model which uses prescribed coefficients is given as,

$$\frac{U(z)}{U^*} = (1 + 0.104Z) - (0.125Z)\exp\left(2.24Z^{0.582}\left(\pm\frac{|z - z_{toe}|}{YZ}\right)\right) \qquad (2)$$

Where $\pm|z - z_{toe}|$ = lateral distance from the toe of slope to the point of interest (positive going towards edge of water and negative over the channel bed), $Y$ = depth of flow over channel bed, $Z$ = cotangent of bank slope, $U(z)$ = depth-averaged velocity and $U^*$ = cross-sectional averaged velocity. Equation (*2*) is modified and improved to model the depth-averaged longitudinal velocity along the channel cross-section for the present meandering trapezoidal channel. As the first step, (*2*) is used for the present channel and departure of the observed depth-averaged velocity points with respect to Wilkerson's model points are shown in Figs.6.1(a, b). The point velocity measurements taken along vertical axes are used to compute depth-averaged velocity at the axis location in one-half trapezoidal channels.

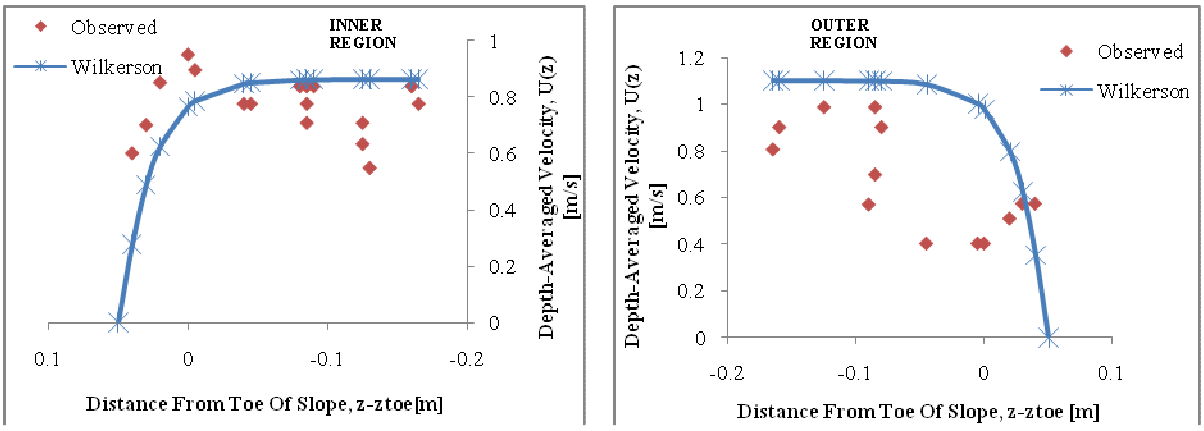


**Fig.6.1 Depth-Averaged Velocity Profile ($Q$ = 14.87 /s, $Y$ = 5cm, $Z$ = 1.0, $S_0$ = 0.0055)**

As shown in Figs. (6.0), the lateral distribution of $U(z)$ predicted by (*2*) does not agree with

the observed data for this wide channel. This deviation ascertains that Wilkerson formula of $U(z)$ for straight trapezoidal channel needs to be modified for present channel to involve meandering effect.

For analysis in meandering channels, the cross-section of the channel is divided along its centreline axis to separate inner and outer regions at the bend apex. Percentage error is calculated for (*2*) and observed values. Figs. 6.2 (a, b) show the percentage error against $\frac{|(z-z_{toe})|}{YZ}$ for inner and outer region of experimental meandering channels. Best fit equations based on regression analysis are used to fit the curve. A second degree polynomial is found as best fit for inner region whereas a third degree for outer region.

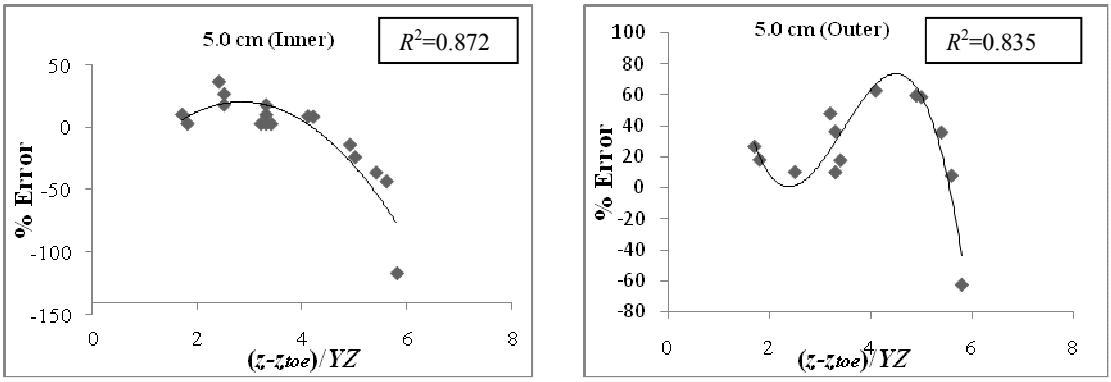


**(a)** **(b)**

**Fig.6.2 Variation of %Error with $(z-z_{toe})/YZ$**

Equation (*2*) is improved to incorporate curvature effect in trapezoidal channel for inner and outer regions respectively to take the form,

$$\left[\left(\frac{U(z)}{U^*}\right)_{inner}\right]_{mod.} = [(1+0.104Z)-(0.125Z)\exp\{2.24Z^{-0.582}*x\}]*[\{0.1098*x^3\}-\{0.6240*x\}+1.6833] \quad (3)$$

$$\left[\left(\frac{U(z)}{U^*}\right)_{outer}\right]_{mod.} = [(1+0.104Z)-(0.125Z)\exp\{2.24Z^{-0.582}*x\}]*[\{0.1548*x^3\}-\{1.599*x^2\}+\{4.991*x\}-3.911] \quad (4)$$

Where, x = ($\pm$| $z-z_{toe}$ |/$YZ$). Fig. (6.1) depicts the comparison of percentage error against | $z-z_{toe}$ |/$YZ$ for three flow depths at the inner region. The trend for various depths is found to be near similar.

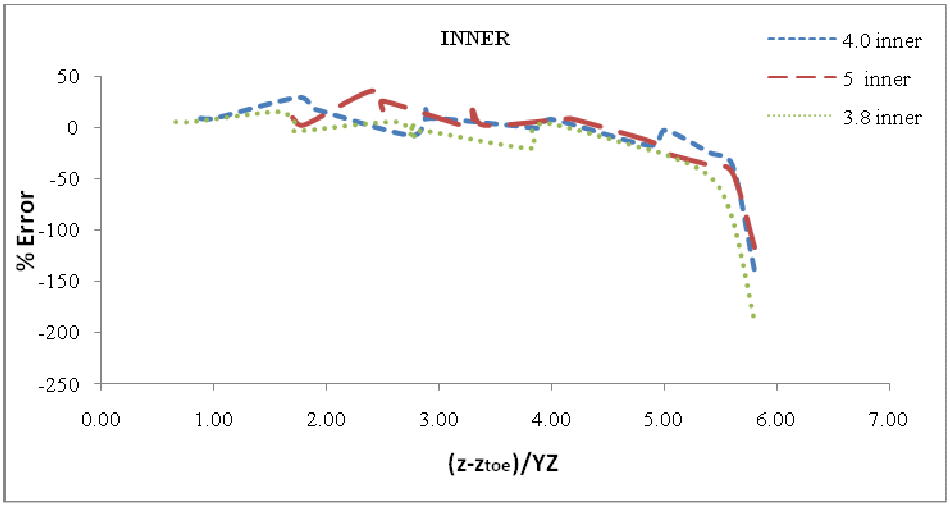


**Fig.6.3 Trends of Plot Between %Error and $(z\text{-}z_{toe})/YZ$ for Three Flow Depths**

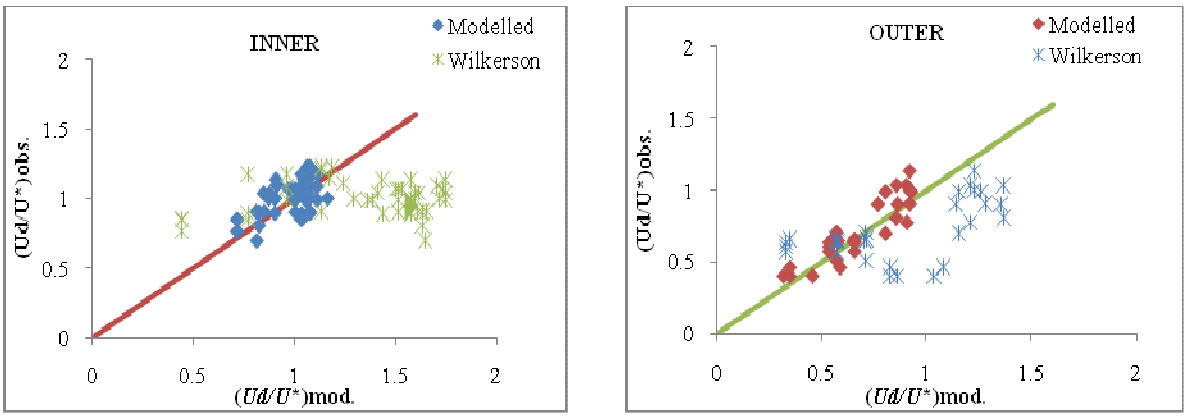


**(a)** **(b)**

**Fig.6.4 Variation of Observed and Modelled Values of ($U_d/U^*$) and its comparison with Wilkerson's Model**

Variation of error in evaluation of $U(z)/U^*$ using modelled equations (3, 4) against observed data for inner and outer regions are presented in Figs.6.4 (a, b). The variation of observed and modelled values as well as Wilkerson model (*2*) and observed values are presented as series1 and series 2 respectively in Fig.6.4. The figures depict least error which shows the sufficiency of developed equation. Also it can be seen that Wilkerson's model deviates at large when incorporated with observed values.

# NUMERICAL MOELING

## 7.1 OVERVIEW

Computational Fluid Dynamics (CFD) is a branch of fluid mechanics that uses numerical methods and algorithms to solve and analyze problems that involve fluid flows. Computers are used to perform the calculations required to simulate the interaction of liquids and gases with surfaces defined by boundary conditions. With high-speed supercomputers, better solutions can be achieved. Ongoing research yields software that improves the accuracy and speed of complex simulation scenarios such as transonic or turbulent flows. It has started around 1960 and with the process of improvement in computer processor speed, CFD simulation is now showing astounding accuracy. The CFD based simulation relies on combined numerical accuracy, modeling precision and computational cost.

The fundamental basis of almost all CFD problems is the Navier–Stokes equations, which define any single-phase fluid flow. These equations can be simplified by removing terms describing viscosity to yield the Euler equations. Further simplification, by removing terms describing vorticity yields the full potential equations. Finally, for small perturbations in subsonic and supersonic flows these equations can be linearized to yield the linearized potential equations. There is no direct solution of the equation for flow. The N-S in vector form for single phase incompressible fluid flow can be expressed as:

$$\frac{\partial}{\partial t}(\rho \bar{u}_i) + \frac{\partial(\rho \bar{u}_i \bar{u}_j)}{\partial z_i} = \frac{\partial}{\partial z_j}\left(\mu \frac{\partial \sigma_{ij}}{\partial z_j}\right) - \frac{\partial \bar{p}}{\partial z_i} - \frac{\partial \tau_{ij}}{\partial z_j} \qquad (5)$$

Where $\sigma_{ij}$ and $\tau_{ij}$ are normal and shear stress component on any assumed plane normal to i along j direction. $\bar{u}_i'$, $\bar{u}_j'$ are time averaged instantaneous velocity component along i,j

directions. p = pressure, μ = co-efficient of viscosity, ρ = density. The process of the numerical simulation of fluid flow using the above equation generally involves four steps and the details are:

(a)Problem identification

1. Defining the modeling goals
2. Identifying the domain to model

(b) Pre-Processing

1. Creating a solid model to represent the domain (Geometry Setup)
2. Design and create the mesh (grid)
3. Set up the physics
    - Defining the condition of flow (e.g turbulent, laminar etc.)
    - Specification of appropriate boundary condition and temporal condition.

(c) Solver

1. Using different numerical schemes to discretize the governing equations.
2. Controlling the convergence by iterating the equation till accuracy is achieved

(d) Post processing

1. Visualising and examining the results
2. Considering revisions to the model

## 7.2 GEOMETRY SETUP

The fluid flow governing equations (momentum equation, continuity equation) are solved based on the discretization of domain using the Cartesian co-ordinate system. This procedure involves dividing the continuum into finite number of nodes. The CFD computations need a spatial discretization scheme and time marching scheme. Mainly the domain discretization is based on Finite element, Finite Volume and Finite Difference Method. Finite Element method is based on dividing the domain into elements. The numerical solution can be obtained in this method by integrating the shape function and weighted factor in an appropriate domain. This method is suitable with respect to both structured and unstructured mesh. The application of Finite Volume method needs dividing the domain into finite number of volumes. Here the specified variables are calculated by solving the discreitized equation in the centre of the cell. This method is developed by taking conservation law in to account. Finite Volume method is suitable for applying in unstructured domain. Finite Difference method is based on Taylor's series approximation. This method is more suitable for regular domain.

The meandering open channel corresponding to one wavelength of five wavelengths is continuously constructed in the experimental flume. In the experimental flume, five meander waves are fabricated for the case of $S_r$ = 1.29, where the sinuosity, $S_r$, is defined as the ratio of the meandering channel length to the meander wavelength. One meander wavelength has trapezoidal cross-section with following dimensions: bed width, 330mm; top width, 460mm; main channel depth, 65mm; meander wavelength, 4054mm and central angle of the bend; 120°. Each section has a 60° circular bend with the centreline radius of 1.1 m followed by a 0.68m

straight reach which approximates a sine generated meandering curve. For the present case of numerical solution, the flow is simulated at 50 mm depth of water in the meander channel.

## 7.3 DISCRETIZATON OF DOMAIN (MESHING)

The discretization of complex computational domain is critical. These kinds of domain don't coincide with the co-ordinate lines with that of a structured grid, which leads to approximation of the geometry. The only procedure to represent complex computational domain is to use a stepwise approximation. But such an approximation is also arduous and quite time consuming. Further, the stepwise approximation introduces truncation error and that can be overcome by providing very fine Cartesian mesh. In whichever way the domain is discretised, based on mesh methods such as any of those mentioned above, care has to be taken in order to produce a good mesh. A mesh with too few nodes could lead to a quick solution, yet not a very accurate one. However a very dense mesh of nodes will potentially waste computational time and memory. Usually more nodes are required within areas of interest, such as near wall and wake regions, in order to capture the large variation of fluid properties expected in these regions. Thus, structure of grid lines causes further wastage of computer storage due to un-necessary refinement. In this study, the flow domain is discretized using structured grid and body-fitted coordinates. The detailed meshing of the flow domain with two views is shown in Fig.7.1

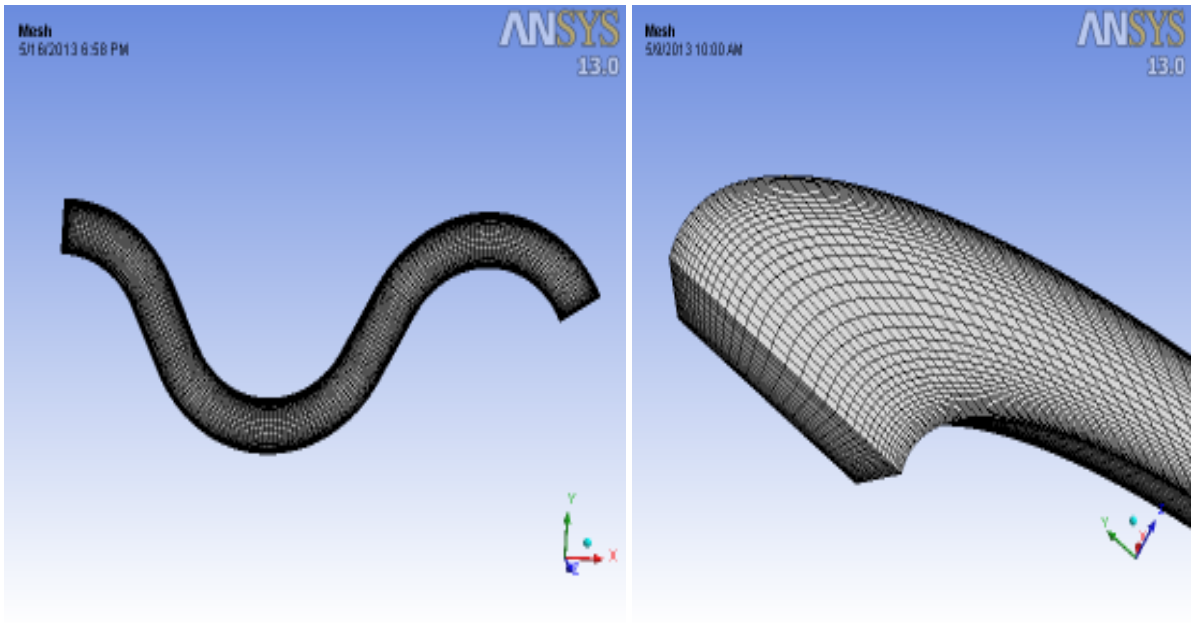


**Fig. 7.1 Schematic diagram of structured mesh**

## 7.4 TURBULENCE

Turbulent flow is a flow regime characterized by chaotic and stochastic property changes. This includes low momentum diffusion, high momentum convection, and rapid variation of pressure and velocity in space and time. Turbulence occurs when the inertia forces in the fluid become significant compared to viscous forces, and is characterized by a high Reynolds Number. In principle, the Navier-Stokes equations describe both laminar and turbulent flows without the need for additional information. However, turbulent flows at realistic Reynolds numbers span a large range of turbulent length and time scales, and would generally involve length scales much smaller than the smallest finite volume mesh, which can be practically used in a numerical analysis. The Direct Numerical Simulation (DNS) of these flows would require computing

power which is many orders of magnitude higher than available in the foreseeable future. To enable the effects of turbulence to be predicted, a large amount of CFD research has concentrated on methods which make use of turbulence models. Turbulence models have been specifically developed to account for the effects of turbulence without recourse to a prohibitively fine mesh and direct numerical simulation. Most turbulence models are statistical turbulence model, as mentioned below.

**Turbulence Models**

- Algebraic (zero-equation) model
- k-ε, RNG k-ε
- Shear stress transport
- k-ω
- Reynolds stress transport model (second moment closure)
- k-ω Reynolds stress
- Detached eddy simulation (DES) turbulence model
- SST scale adaptive simulation (SAS) turbulence model
- Smagorinsky large eddy simulation model (LES)
- Scalable wall functions
- Automatic near-wall treatment including integration to the wall
- User-defined turbulent wall functions and heat transfer

The two exceptions to this in ANSYS CFX are:

• Large Eddy Simulation Theory

• Detached Eddy Simulation Theory

However open-channel flows are characterized by complicated flow structures, even for simple geometry, such as that of a rectangular channel. This is largely due to wall and free surface boundaries. The secondary currents are generated in open channel flow because free surface and walls reduce the turbulence intensity in the direction normal to the surface or the walls and lead to anisotropy of turbulence. The three dimensional nature of turbulent flow can be decomposed into mean part and fluctuation part, which is called Reynolds decomposition. Gravity and channel geometry are mainly responsible for turbulent flow for this particular condition.

## 7.5 NUMERICAL MODEL

### *7.5.1 Large Eddy Simulation (LES)*

The three major types of turbulence methodologies are Direct Numerical Simulation (DNS), Large eddy Simulation (LES) and k-ε modelling. k-ε models the turbulent flows by time or space averaging. But it is not suitable for transient flows because the averaging process removes most of the important characteristics of a time-dependent solution. On the other hand, Direct Numerical Simulation, attempts to solve all time and spatial scales. As a result, the solution is very accurate. However to resolve almost all ranges of scales, the spatial and temporal grids would need to be extremely small in the order of Kolmogorov length and time scale, resulting in a problem which would take an extraordinarily long time to solve, making it computationally intensive.

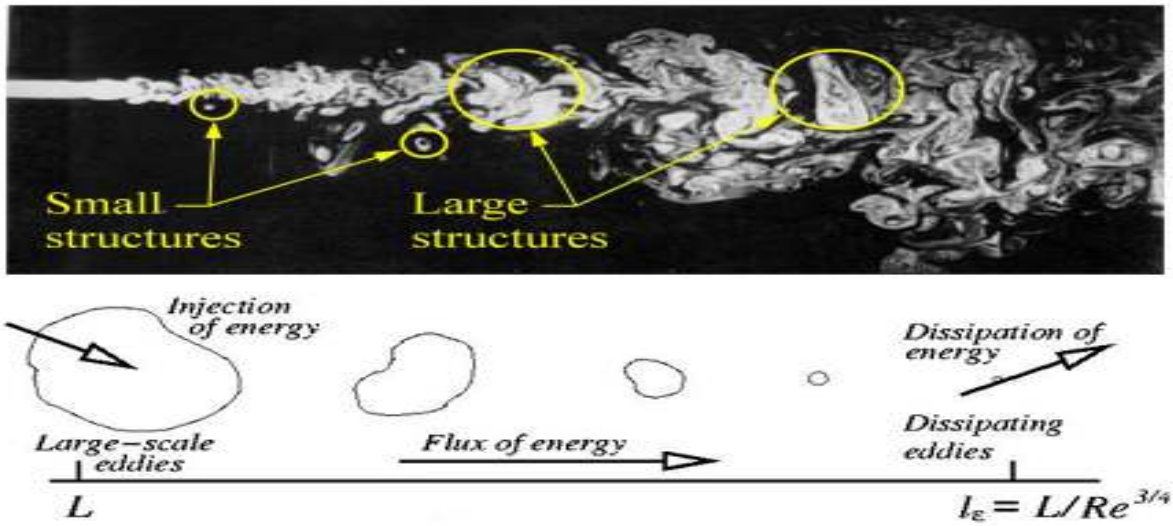


**Fig. 7.2 Energy cascade process with length scale**

One compromise between these two models is Large Eddy Simulation. Large Eddy Simulation directly solves large spatial scales (DNS), while modeling the smaller scales (k-epsilon). First, the larger scales that carries the majority of the energy, which accounts for 80% of turbulent flow energy and hence is more important. Second, the smaller scales have been found to be more universal, and hence are more easily modeled. The resulting methodology is a hybrid between these two methods, which involves the filtering of the Navier-Stokes equations to separate those scales which will be modeled from those which will be solved for directly. Subsequently LES method simulates large scale turbulent motions directly, while the unresolved small scale motions are modeled through the use of a Smagorinsky model. This model captures larger scale motion such as DNS, as well as it covers the effects of small scales of eddies by using sub-grid scale (SGS) model.

### *7.5.2 Mathematical Model*

Large Eddy Simulation (LES) is about filtering of the equations of movement and decomposition of the flow variables into a large scale (resolved) and a small scale (unresolved) parts. Any flow variable f can be written such as:

$$f = \overline{f} + f' \tag{6}$$

Where $\overline{f}$ the large scale part, is defined through volume averaging as:

$$\overline{f}(x_i, t) = \int_{Vol} G(x_i - x_i') f(x_i', t) dx_i' \tag{7}$$

Where, G(x –$x'$) is the filter function (called the hat filter or Gaussian filter). After performing the volume averaging and neglecting density fluctuations, the filtered Navier-Stokes equations become:

$$\frac{\partial(\rho \overline{U_i})}{\partial t} + \frac{\partial(\rho \overline{U_i U_j})}{\partial x_j} = -\frac{\partial \bar{p}}{\partial x_i} + \mu \frac{\partial^2 \overline{U_i}}{\partial x_j \partial x_j} \tag{8}$$

The non linear transport term in the filtered equation can be developed as:

$$\overline{U_i U_j} = \overline{(\overline{U_i} + u_i')(\overline{U_j} + u_j')} = \underset{(1)}{\overline{\overline{U_i}\,\overline{U_j}}} + \underset{(2)}{\overline{\overline{U_i} u_j'}} + \underset{(3)}{\overline{\overline{U_j} u_i'}} + \underset{(4)}{\overline{u_i' u_j'}} \tag{9}$$

In time, averaging the terms (2) and (3) vanish, but when using volume averaging, this is no longer true.

Introducing the sub-grid scale (SGS) stresses, $\tau_{ij}$, as:

$$\tau_{ij} = \overline{u_i u_j} - \overline{U_i}\,\overline{U_j} \tag{10}$$

we can rewrite the filtered Navier-Stokes equations as:

$$\frac{\partial(\rho\overline{U_i})}{\partial t}+\frac{\partial(\rho\tau_{ij}+\rho\overline{U_i}\overline{U_j})}{\partial x_j}=-\frac{\partial\bar{p}}{\partial x_i}+\mu\frac{\partial^2\overline{U_i}}{\partial x_j\partial x_j} \tag{11}$$

$$\frac{\partial(\rho\overline{U_i})}{\partial t}+\frac{\partial(\rho\overline{U_i}\overline{U_j})}{\partial x_j}=-\frac{\partial\bar{p}}{\partial x_i}+\mu\frac{\partial^2\overline{U_i}}{\partial x_j\partial x_j}-\frac{\partial(\rho\tau_{ij})}{\partial x_j} \tag{12}$$

with

$$\tau_{ij}=\overline{u_iu_j}-\overline{U_i}\,\overline{U_j}=\overline{\overline{U_i}\,\overline{U_j}}+\overline{\overline{U_i}u_j'}+\overline{\overline{U_j}u_i'}+\overline{u_i'u_j'}-\overline{U_i}\,\overline{U_j}=L_{ij}+C_{ij}+R_{ij}$$

$$C_{ij}=\overline{\overline{U_i}u_j'}+\overline{\overline{U_j}u_i'}=\text{Cross Terms}$$

Above equation is the basis of the LES technique. LES explicitly models smaller scale motions thereby reducing the computational cost to a larger extent than DNS in which effort is given in modeling smaller scales whereas larger scales predominantly contains energy and anisotropy.

**Sub-Grid Scale Models**

The non-linear transport of energy generates ever-smaller scales like a cascade process until it reaches the size of Kolmogorov scales as shown in Fig.7.2. The essence of LES is to account for this energy cascade from resolved large scales to the unresolved sub-grid scales. This is the role of the SGS model. The most popular class of SGS models is the eddy-viscosity type, based on (variants of) the Smagorinsky model (Smagorinsky, 1963).

**Smagorinsky Model**

The Smagorinsky model can be thought of as combining the Reynolds averaging assumptions given by $L_{ij} + C_{ij} = 0$ with a mixing-length based eddy viscosity model for the Reynolds SGS tensor. It is thereby assumed that the SGS stresses are proportional to the modulus of the strain rate tensor, $\overline{S_{ij}}$ of the filtered large-scale flow:

$$\tau_{ij} - \frac{1}{3}\tau_{kk} = -2 \cdot \nu_{SGS} \cdot \bar{S}_{ij} = -\nu_{SGS} \cdot \left( \frac{\partial \overline{U_i}}{\partial x_j} + \frac{\partial \overline{U_j}}{\partial x_i} \right) \quad (13)$$

To close the equation, a model for the SGS viscosity $V_{SGS}$ is needed. Based on dimensional analysis, the SGS viscosity can be expressed as:

$$\nu_{SGS} \propto l \, q_{SGS} \quad (14)$$

Where l is the length scale of the unresolved motion (usually the grid size $\Delta = (\text{vol})^{1/3}$ ) and $q_{SGS}$ is the velocity of the unresolved motion. In the Smagorinsky model, based on an analogy to the Prandtl mixing length model, the velocity scale is related to the gradients of the filtered velocity:

$$q_{SGS} = \Delta|\bar{S}| \text{ Where } \quad |\bar{S}| = (2\bar{S}_{ij}\bar{S}_{ij})^{1/2} \quad (15)$$

This yields the Smagorinsky model for the SGS viscosity:

$$\nu_{SGS} = (C_S\Delta)^2|\bar{S}| \quad (16)$$

With $C_s$ the Smagorinsky constant. The value of the Smagorinsky constant for isotropic turbulence with inertial range spectrum:

$$E(k) = C_k\varepsilon^{2/3}k^{-5/3} \text{ is } C_S = \frac{1}{\pi}\left(\frac{2}{3C_k}\right)^{3/4} = 0.18 \quad (17)$$

For practical calculations, the value of $C_s$ is changed depending on the type of flow and mesh resolution. Its value is found to vary between a value of 0.065 (channel flows) and 0.25. Often a value of 0.1 is used.

## 7.6 BOUNDARY CONDITIONS

### *7.6.1 Wall*

A no-slip boundary condition is the most common boundary condition implemented at the wall and prescribes that the fluid next to the wall assumes the velocity at the wall, which is zero.

$U = V = W = 0$

### *7.6.2 Free Surface*

Here, Symmetry Boundary condition is used for the free-surface. This condition follows that, no flow of scalar flux occurs across the boundary. In applying this condition normal velocities are set to zero and values of all other properties outside the domain are equated to their values at the nearest node just inside the domain. Here the experimental bulk velocity of the flow is initially approximated as:

$W$ = 0.319 m/s, $V = 0$, $U = 0$ and $\frac{\partial w}{\partial z} = 0$

### *7.6.3 Inlet and Outlet Boundary Condition*

To initialize the flow a mean velocity was specified over the whole inlet plane and is computed by $U_{in}=Q/A$, where $Q$ is the flow discharge of the channel and $A$ is the cross section area of the inlet. A pressure gradient was further specified across the domain to drive the flow. In order to specify the pressure gradient the channel geometries were all created flat and the effects of gravity and channel slope implemented via a resolved gravity vector. It represents the angle between the channel slope and the horizontal, the gravity vector is resolved in x, y and z components as ($\rho g sin\theta \;\; 0 \;\; -\rho g cos\theta$).

Where $\theta$ = angle between bed surface to horizontal axis. Here, the $x$ component denotes the direction responsible for flow of water along the channel and the z component is responsible for creating the hydrostatic pressure. From the simulation, $z$ component of the gravity vector ($-\rho g\cos\theta$) is found to be responsible for the convergence problem of the solver.

Opening type boundary condition is imposed at the outlet.

## 7.7 NUMERICAL RESULTS

ANSYS-CFX 13.0 solver manager is used to carry out the simulation process. Here the advection term is discretized with bounded central difference scheme and transient terms are discretized with Second order scheme. Courant number ($C_r$) is controlled between 0 - 0.5. After that, the equation is iterated over and over till desirable level of accuracy of $10^{-6}$ of residual value is achieved.

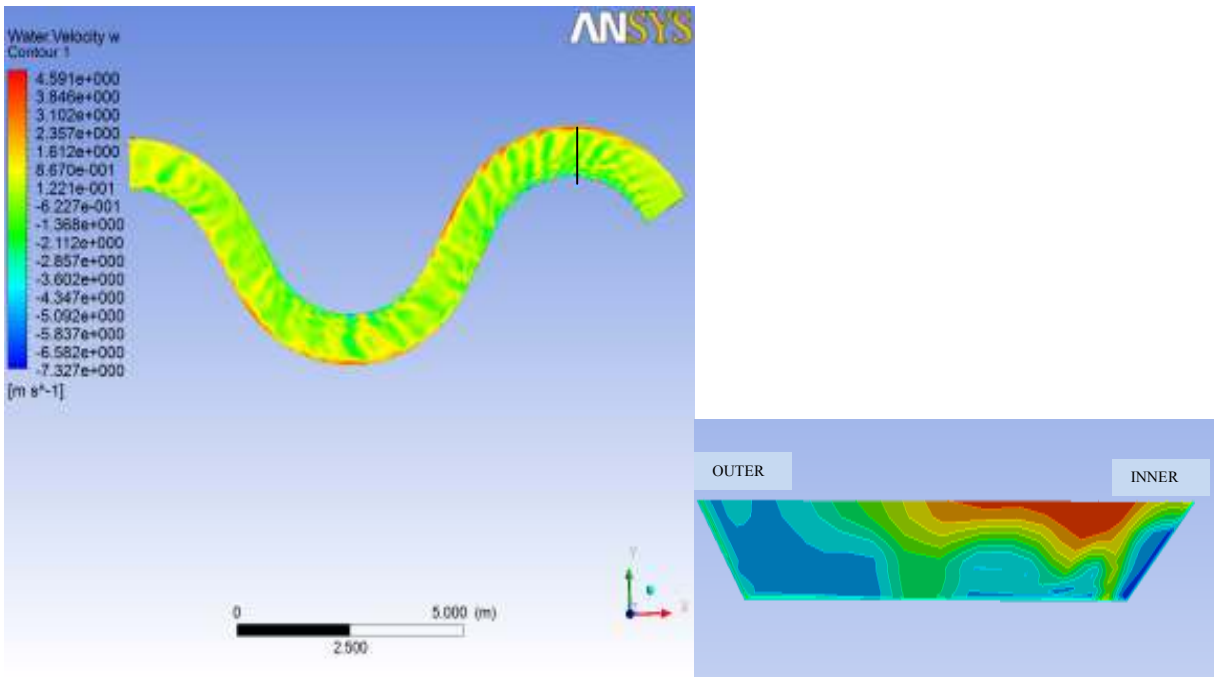


**(a) Longitudinal (tangential) Velocity Contour with cross section at the third bend apex**

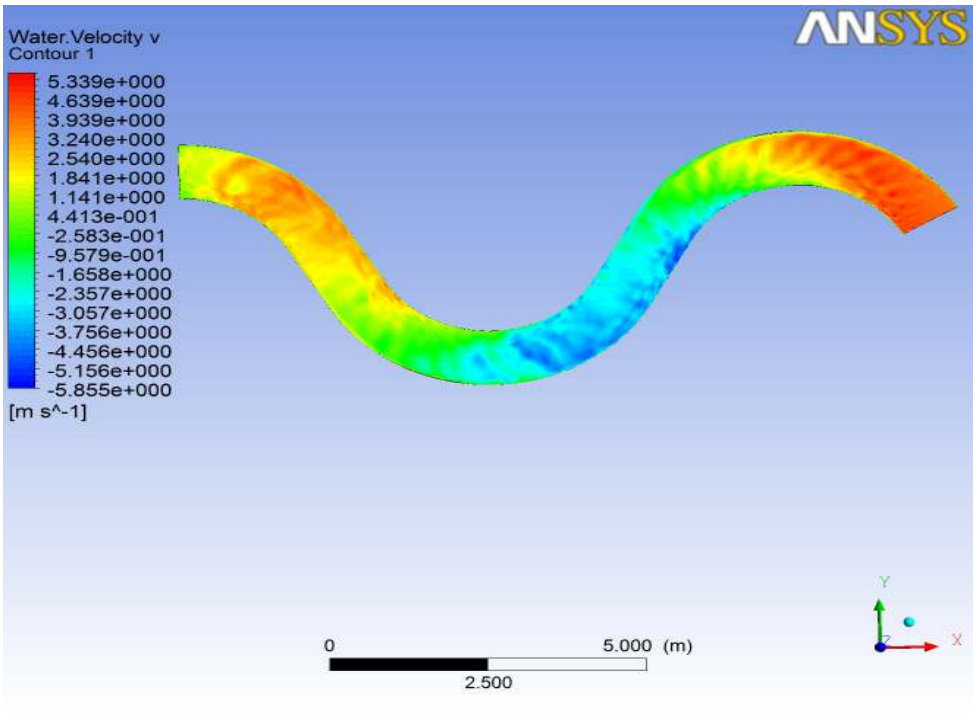


**(b) Lateral (radial) Velocity Contour**

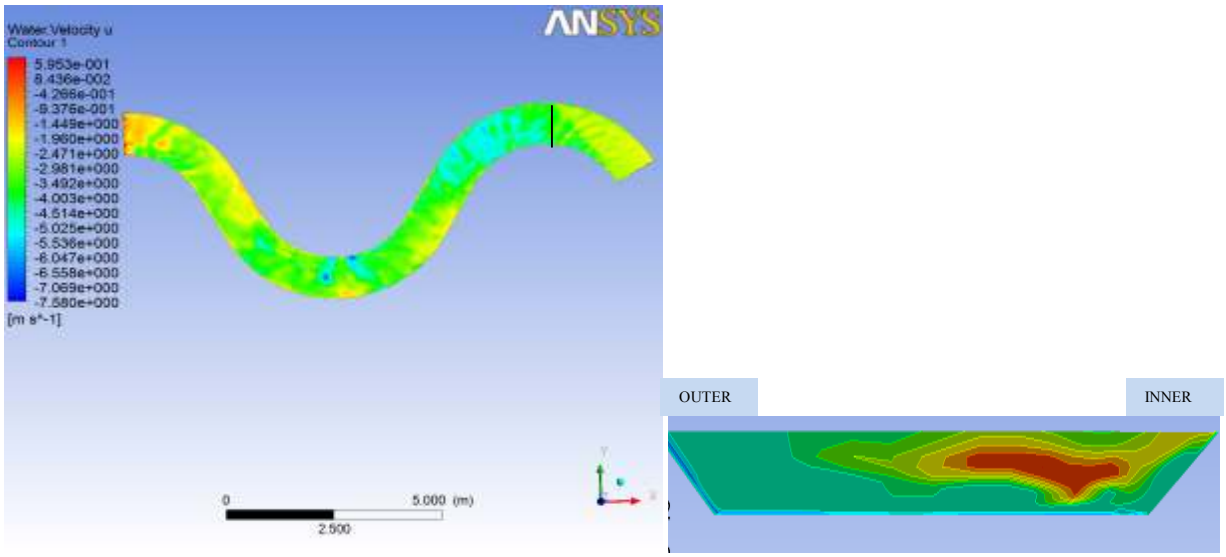


**(c) Vertical Velocity Contour with cross section at the third bend apex**

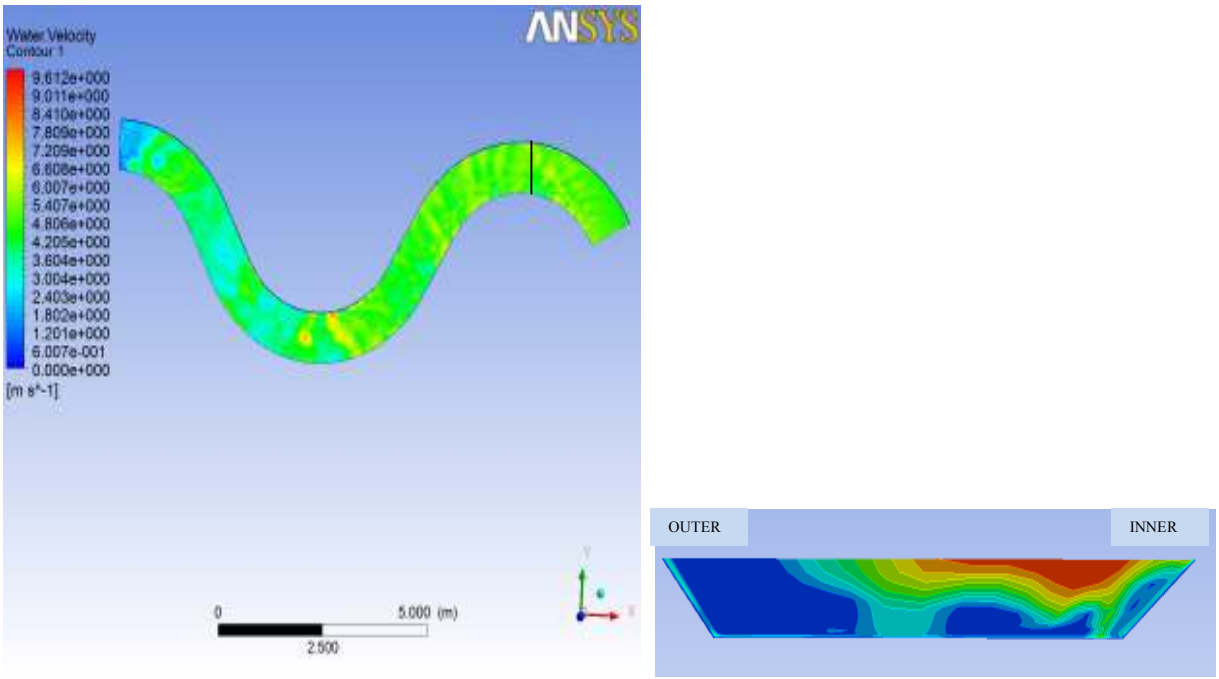


**(d) Resultant Velocity Contour with cross section at the third bend apex**

**Fig. 7.3 Velocity Contours developed by ANSYS CFX**

The velocity is simulated for the 60 degree simple meandering channel. The simulation results show that the flow patterns are similar to experimental studies. Figure 7.3 shows the contours of tangential, radial and vertical velocity at the free surface and also the resultant velocity at the free surface are shown in this figure.

Tominaga and Nezu (1991) noticed that the flow is considered to be uniform incompressible fully developed turbulent flow at a test section of 7.5 m. So to incorporate this length, a cross sectional plane is extracted at the third bend apex where the pattern of velocity distribution is studied for present analysis. The contours of experimental velocity as shown in Figures 4.2 (a)-4.3(d) depicts the presence of maximum thread of velocity values towards the inner region of the trapezoidal channel whereas the concentration of minimum velocity is mostly confined to the

outer regions, as such the modeled velocity reveals almost the same distribution pattern as given in Figure 7.3. Another feature which is discernible from the experimental velocity contour is that the maximum velocity lies towards the inner free surface which is also marked in the velocity contours of numerically modeled trapezoidal cross section. It is seen that the numerical simulation is in reasonable agreement with the experimental measurements.

# CONCLUSIONS AND FURTHER WORK

## 8.1 CONCLUSIONS

The present theoretical investigation supported by experimental observation is made for meandering channels with and without floodplains having different flow aspect ratios. On the basis of the investigations concerning flow, velocity distribution, and depth average velocity distribution in smooth open compound channels, the following conclusions are drawn.

1. The model for depth-averaged velocity distribution proposed by Wilkerson (2005) does not fit to meandering channels. The modelled equations (3, 4) which include the influencing dimensionless channel parameters are found to be adequate for the present set of simple meander channel data and can be used to compute the depth average velocity across the channel cross sections.
2. For simple meandering channel, normalised depth-averaged velocities ($U_d/U^*$) at the inner wall are found to be higher than the outer wall in the meandering channel contrary to straight channels (Wilkerson *et.al*., 2005).
3. The depth averaged velocity is found to be maximum (Fig. 5.2) along the centre line axis of simple meander channel at the bend apex. This is in line with the observations for natural straight and curved channels. As one move from centre line towards the channel corner, decrease in the depth average velocity is marked and the maximum decrease is observed at the region of nearly 25% of radial distance from the centre line of meander channel, both in the inner and outer directions. The rate of decrease is faster for lower depths of flow than for higher depths.
4. In compound meander channel, the higher values of depth averaged velocity are found at the inner flood plain region and attain a maximum value at the junction between the main channel bank and the flood plain. It can also be seen that the

minimum depth average velocity values occurred at the junctions between the bed and the outer bank of main channel.

5. As shown in the experimental velocity contours, the numerical velocity contours also give the same result. The presence of maximum thread of velocity values towards the inner region of the trapezoidal channel whereas the concentration of minimum velocity is mostly confined to the outer regions. The maximum velocity lies towards the inner free surface which is also marked in the velocity contours of numerically modelled trapezoidal cross section. It is seen that the numerical simulation is in reasonable agreement with the experimental measurements.

## 8.2 FUTURE SCOPE OF WORK

The present work leaves a wide scope for future investigators to explore many other aspects of compound channel analysis.

1. The result can be compared with data of straight channel and further the work can be extended to natural channels and other laboratory channels with different sinuosity, geometry and surface conditions.
2. Further investigations can be done to study depth-averaged velocity in vertical and lateral directions and develop models using analytical and numerical approaches which are more convenient than conventional methods.
3. Velocity profiles can be drawn in transverse direction, the type of wall law that coexists at inner and outer wall of meandering channels can be defined and velocity dip phenomenon can be studied.
4. The accretion in 3D flow structure is obvious when water overtops the bank to flow in flood plains as mostly seen in natural rivers during flood, which is commonly modelled as compound channel in laboratory. Thus a model can be proposed to evaluate velocity distribution in compound channel incorporating turbulence effects.

5. Proceedings on lateral velocity distribution can be done on mobile bed to represent real situation prevailing in natural rivers; so that sediment load transport and boundary shear distribution can be determined to its accuracy.
6. Further investigations can be done to study stream wise depth-averaged velocity and develop models using analytical and numerical approaches which are more convenient than conventional methods.

# REFERENCES


1. Afzal, N., Seena A., Bushra A.2007. Power law velocity profile in fully developed turbulent pipe and channel flows. J. Hydr. Engrg , Vol. 133, No. 9, 1080-1086.
2. Ahmadi, M. M., Ayyoubzadeh, S. A., Montazeri Namin, M., and Samani, J. M. V.,2009. A 2D Numerical Depth-averaged Model for Unsteady Flow in Open Channel Bends. J. Agr. Sci. Tech. Vol. 11: 457-468.
3. Albayrak, I., and Lemmin, U. 2011. Secondary Currents and Corresponding Surface Velocity Patterns in a Turbulent Open-Channel Flow over a Rough Bed. J. Hydr. Engrg. ,Vol. 137, No. 11, 1318 – 1334.
4. Beaman F.(2010). Large Eddy Simulation of open channel flows for conveyance estimation. Ph.D thesis, University of Nottingham.
5. Boussinesq, J. (1868). Mémoire sur l'influence des frottements dans les mouvements reguliers des fluids. J. Math. Pures Appl. (2me sér.), 13, 377-424.
6. Cater, J.E., and Williams, J.R. 2008. Large eddy simulation of a long asymmetric compound open channel. *Journal of Hydraulic Research*. Vol. 46(4).
7. Celik I, Rodi W. Modeling suspended sediment transport in non-equilibrium situation. Journal of Hydraulic Engineering (ASCE) 1988; 114:1157 – 1191.
8. Cokljat D, Younis BA. Second-order closure study of open channel flows. Journal of Hydraulic Engineering (ASCE) 1995; 121:94 – 107.
9. Coleman, N. L. (1981). Velocity profiles with suspended sediment. J. Hydr. Res, 19(3), 211-229.
10. Coles, D. 1956.The law of the wake in the turbulent boundary layer. J. Fluid Mech., 1,191-226.

11. Ervine, D.A., et al. 2000. Two-Dimensional solution for straight and meandering overbank flows. J. Hydr. Engrg , Vol. 126, No. 9, 0653-0669.
12. Jia, Y., Blanckaert, K. & Wang, S.S. 2001. Numerical simulation of secondary currents in curved channels. Proc. 8th FMTM-congress, Tokyo.
13. Johannesson, H. and Parker, G. 1989. Velocity Redistribution in Meandering Rivers. J. Hydr. Engrg , Vol. 115, No. 8, 0008-1019.
14. Jing, H., Guo, Y., Li, C., & Zhang, J. 2009. Three dimensional numerical simulation of compound meandering open channel flow by the Reynolds stress model. *International Journal for Numerical Methods in Fluids*, 59, 927-943.
15. Kang H, Choi SU. (2006) "Reynolds stress modeling of rectangular open-channel flow." *International Journal for Numerical Methods in Fluids 2006;* 51:1319 – 1334.
16. Kirkgoz, M.S. et al. 1997. Velocity Profiles of Developing and Developed Open Channel Flow. J. Hydr. Engrg , Vol. 123, No. 12, 1099-1105.
17. Knight, D.W., et al. 2007. Modelling Depth-Averaged Velocity and Boundary Shear in Trapezoidal Channels with Secondary Flows. J. Hydr. Engrg , Vol. 133, No. 1, 1-39– 47.
18. Kundu .S and Ghoshal .K., 2010. Velocity Distribution in Open Channels: Combination of Log-law and Parabolic-law. World Academy of Science, Engineering and Technology 68 2012.
19. Launder BE, Spalding DB.1974. The numerical computation of turbulent flows. Computer Methods in *Applied Mechanics and Engineering 1974; 3:269 – 289.*
20. Orgaz, O.C. 2010. Velocity Profile and Flow Resistance Models for Developing Chute Flow. J. Hydr. Engrg , Vol. 136, No. 7, 7-447– 452.
21. Maria, A.A, and DaSilvaA. F.1999. Friction Factor of Meandering Flows. Journal of Hydraulic Engineering, ASCE, Vol.125, No.7, pp. 779-783.

22. Myers, W.R.C. (1987. Velocity and Discharge in Compound Channels. Journal of Hydraulic Engineering, ASCE, Vol.113, No.6, pp. 753-766.
23. Patra, K.C. 2004. Flow and Velocity Distribution in Meandering Compound Channels. J. Hydr. Engrg , Vol. 130, No. 5, 5-398 – 411.
24. Pezzinga, G. 1994. Velocity Distribution in Compound Channel Flows by Numerical Modeling. . Hydr. Engrg , Vol. 120, No. 10, 0010-1176.
25. Prandtl, L.1932. Recent Results of Turbulent Research, translation by National Advisory Committee for Aeronautics, TM No. 720 (originally published in German in 1933).
26. Rameshwaran P, Naden PS.2003. Three-dimensional numerical simulation of compound channel flows." Journal of Hydraulic Engineering (ASCE) 2003; 129:645 – 652.
27. Salvetti MV, Zang Y, Street RL and Banerjee S. 1997. Large-eddy simulation of free surface decaying turbulence with dynamic subgrid -scale models. Physics of Fluids. 9, pp. 2405.
28. Sarma, N.V.K., Prasad R.V.B., Sarma K.A. (2000). "Detailed study of binary law for open channel." J. Hydr. Engrg., Vol. 126, No. 3,210-214.
29. Sugiyama H, Hitomi D, Saito T. 2006. Numerical analysis of turbulent structure in compound meandering open channel by algebraic Reynolds stress model. *International Journal for Numerical Methods in Fluids* 2006; 51:791 – 818.
30. Tang, X. And Knight, D.W. 2008. A general model of lateral depth-averaged velocity distributions for open channel flows. J. Hydr. Engrg., Vol. 134, No. 9, 1337-1342.
31. Tominaga, A., Nezu I.1992. Velocity profiles in steep open-channel flows. J. Hydr. Engrg., Vol. 118, No. 1, 73-90.
32. Thomas TG. and Williams J.1995a. Large eddy simulation of a symmetric trapezoidal channel at Reynolds number of 430,000. J. Hydraul. Res.. 33(6), pp. 825-842.

33. Thomas TG. and Williams J.1995b. Large eddy simulation of turbulent flow in an asymmetric compound open channel. J. Hydraul. Res. 33(1), pp. 27-41.
34. Thomas TG. and Williams J.1999. Large eddy simulation of flow in a rectangular open channel. J. Hydraul Res. 37(3), pp. 345-361.
35. Willetts, B.B., and Hardwick, R.I. 1993. Stage Dependency for Over Bank Flow in Meandering Channels. Proceedings of the Institution of Civil Engineers, Water, Maritime and Energy, March, Vol.101, paper No.10049, 45-54.
36. Wilkerson, V.G., McGahan J.L.2005. Depth averaged velocity distribution in straight trapezoidal channel. J. Hydr. Engrg, Vol. 131, No. 6, 509-512.
37. Wormleaton, P. R., and Hadjipanos, P. 1985. ‘‘Flow distribution in compound channels.’’ J. Hydr. Div., Vol. 111, No. 2, 357–361.
38. Yang K, Cao S, and Liu X. 2007.Flow resistance and its prediction methods in compound channels, Acta Mechanic Sinica; 21, pp.353-61Yen BC. (2002). Open flow resistance. J. Hydr. Eng, 1(20), pp.20-39.
39. Zarrati, A.R., Tamai, N., and Jin, Y.C.2005. Mathematical Modeling of Meandering Channels with a Generalized Depth Averaged Model. Journal of Hydraulic Engineering, ASCE, Vol.131, No.6, pp. 467-475.

## Publications from the Work

### A: Published

1. Mohanty, L., Patra.K.C., Khatua, K.K., Patnaik, M. (2012) "Depth-Averaged Velocity Distribution in Trapezoidal Meandering Channels" Proceedings of National Conference on Hydraulic and Water Resources, IIT Bombay, India, HYDRO 2012, 625-634.
2. Patnaik, M., Patra.K.C., Khatua, K.K., Mohanty, L. (2012) "Boundary Shear Distribution in Highly Sinuous Meandering Channels" Proceedings of National Conference on Hydraulic and Water Resources, IIT Bombay, India, HYDRO 2012, 1233-1242.
3. Mohanty, L., Patnaik, M., Patra.K.C. (2013) "Lateral Distribution of Depth-Averaged Velocity in Trapezoidal Meandering Channels" Symposium on Sustainable Infrastructure Development, IIT, Bhubaneswar, Odisha, India, IWMSID 2013, 383-389.
4. Patnaik, M., Mohanty, L., Patra.K.C. (2013) "Wall and Bed Shear Distribution in Meandering Channels" Symposium on Sustainable Infrastructure Development, IIT, Bhubaneswar, Odisha, India, IWMSID 2013, 374-382.

### B: Accepted for Publication

1. Mohanty, L., Patra.K.C., Khatua, K.K., Patnaik, M. (2012) "Modeling Depth-Averaged Velocity in Trapezoidal Meandering Channels" accepted for ISH *Journal of Hydraulic Engineering,* Taylor & Francis Group, UK.
2. Patnaik, M., Patra.K.C., Khatua, K.K., Mohanty, L. (2012) "Modeling Boundary Shear Stress in Highly Sinuous Meandering Channels" accepted for ISH *Journal of Hydraulic Engineering,* Taylor & Francis Group, UK.